REPORT DOCUMENTATION PAGE

The public reporting burden for this collection of information is estimated to average 1 hour per response, including the time for reviewing instructions, searching existing data sources, gathering and maintaining the data needed, and completing and reviewing the collection of information. Send comments regarding this burden estimate or any other aspect of this collection of information, including suggestions for reducing this burden, to Department of Defense, Washington Headquarters Services, Directorate for Information Operations and Reports (0704-0188), 1215 Jefferson Davis Highway, Suite 1204, Arlington, VA 22202-4302. Respondents should be aware that notwithstanding any other provision of law, no person shall be subject to any penalty for failing to comply with a collection of information if it does not display a currently valid OMB control number.
PLEASE DO NOT RETURN YOUR FORM TO THE ABOVE ADDRESS.

1. REPORT DATE (DD-MM-YYYY)	2. REPORT TYPE	3. DATES COVERED (From - To)
31-03-2011	Final Report	June 28, 2010 - October 31, 2010

4. TITLE AND SUBTITLE

Dynamic Microstructure Design Consortium

5a. CONTRACT NUMBER

N00014-10-M-0333

5b. GRANT NUMBER

5c. PROGRAM ELEMENT NUMBER

6. AUTHOR(S)

Olson, Gregory B.

5d. PROJECT NUMBER

5e. TASK NUMBER

0001AB

5f. WORK UNIT NUMBER

7. PERFORMING ORGANIZATION NAME(S) AND ADDRESS(ES)

QuesTek Innovations LLC
1820 Ridge Avenue
Evanston, IL 60201

8. PERFORMING ORGANIZATION REPORT NUMBER

ONR01-018 Final Report

9. SPONSORING/MONITORING AGENCY NAME(S) AND ADDRESS(ES)

Office of Naval Research
875 North Randolph St.
Arlington, VA 22203-1995

10. SPONSORING/MONITOR'S ACRONYM(S)

Office of Naval Research

11. SPONSORING/MONITORING REPORT NUMBER

12. DISTRIBUTION/AVAILABILITY STATEMENT

DISTRIBUTION A. Approved for public release: distribution unlimited

13. SUPPLEMENTARY NOTES

14. ABSTRACT

Anticipating the computational power advances over the next decade, we have assessed and prioritized the enabling fundamental research tools offering the broadest impact in computational materials engineering, with emphasis on the context of ongoing near- and long-term alloy development efforts for Navy applications. Exploiting practical use cases to motivate tool utility and define required computational efficiency, our goal was an integrated set of flexible, high fidelity validated simulation and tomographic characterization tools for 3D microstructural evolution in both processing and service in support of process/structure and structure/property modeling for both materials design and development. Through close collaboration of computational engineering companies with tool users we also sought rapid commercially supported dissemination of these new capabilities.

15. SUBJECT TERMS

D3D, 3D microstructure, computational models

16. SECURITY CLASSIFICATION OF:			17. LIMITATION OF ABSTRACT	18. NUMBER OF PAGES	19a. NAME OF RESPONSIBLE PERSON
a. REPORT	b. ABSTRACT	c. THIS PAGE			Gregory B. Olson, Sc.D.
U	U	U	UU	64	19b. TELEPHONE NUMBER (Include area code) (847) 425-8220

TITLE: Dynamic Microstructure Design Consortium

AUTHOR: **Gregory B. Olson, Professor**

COMPANY NAME: **QuesTek Innovations LLC**

COMPANY ADDRESS: **1820 Ridge Avenue**
                        Evanston, IL 60201-3621

DATE: **March 23, 2011**

Final Report: **Contract No. N00014-10-M-0333**

Executive Summary

A suite of tomographic characterization and analysis tools for quantification of the spatial distribution of multiscale particle dispersions has been integrated with a set of high fidelity 3D simulation tools addressing microstructural evolution governing strength, toughness, shear instability resistance and fatigue strength in high-performance steels for naval applications. Atomic-scale LEAP tomographic reconstruction has quantified the obstacle spacing distributions in martensitic steels strengthened by a combination of bcc Cu and M_2C carbide precipitation. Numerical simulation of dislocation motion in these microstructures quantifies the role of measured spatial nonuniformity and nonlinear superposition behavior. Collaborative FIB/SEM reconstruction of submicron TiC grain refining carbide dispersions has quantified their spatial inhomogeneity. Adapting a multipole diffusion method to the 3D simulation of precipitation processes predicts similar spatial nonuniformity for both the nanoscale bcc Cu strengthening dispersion and the submicron TiC grain refining dispersion, arising from the distributed nature of multiparticle diffusion field interactions. FIB/SEM reconstruction of submicron TiC dispersions in a shear band cut from an isothermal shear test specimen taken to the onset of shear localization demonstrates an early stage of microvoid formation at TiC particle clusters. Direct simulation of microvoiding at TiC clusters taken from tomographic reconstructions predicts an important role of clustering in the initiation of microvoid softening driven shear localization. Reconstruction of the martensite packet structure surrounding the observed microvoid cluster supports an important role of crystal plasticity predicted by simulations. A concurrent multiscale constitutive model combining the effects of submicron microvoiding and coarser primary voiding on multi-micron scale inclusions allows parametric toughness modeling, predicting an important role of interfacial adhesion for both particle populations. Rigorous FLAPW quantum mechanical calculations address 3D issues in the adhesion of these interfaces. Slab calculations compare interfacial bonding strength in coherent patches of Fe/MX metal carbonitride interfaces for the (Ti,V,Nb.Mo,Al)(C,N) system. Larger cell calculations quantify the reduction of interfacial adhesion by a hierarchy of intrinsic defects including primary interfacial dislocations and atomic steps. Bond topological analysis of computed charge densities quantifies bond breaking processes during interfacial fracture and predicts an important role of Fe-Fe second neighbor bonding influenced by alloying. The prediction of a beneficial effect of matrix Ni alloying is validated by FLAPW calculations. Light microscopy based tomographic reconstruction quantifies the distribution of primary inclusions based on nitrides, oxides and sulfides, including oxysulfide clusters identified as the most potent fatigue nucleation sites in high-performance gear steels. Crack tip reconstruction clarifies the relation of primary voids and the pattern of shear localization that accelerates their coalescence, consistent with an observed correlation of normalized toughness with critical void growth ratio. Femtosecond laser (FSL) tomography demonstrates the capability to more rapidly section larger representative volumes for primary inclusion distribution reconstruction. Numerical simulation of 3D cyclic deformation processes at reconstructed inclusion clusters predict a dominant role of prior interfacial damage in defining the potency of observed fatigue nucleation sites, while direct simulation of particle pair interactions predicts high anisotropy of fatigue strength based on the observed orientation of inclusion clusters. Use cases of the new techniques have addressed a range of high-performance steels of naval interest, and have played an important supporting role in several Navy sponsored SBIR/STTR alloy design projects.

Table of Contents

Introduction

Anticipating the computational power advances over the next decade, we have assessed and prioritized the enabling fundamental research tools offering the broadest impact in computational materials engineering, with emphasis on the context of ongoing near- and long-term alloy development efforts for Navy applications. Exploiting practical use cases to motivate tool utility and define required computational efficiency, our goal was an integrated set of flexible, high fidelity validated simulation and tomographic characterization tools for 3D microstructural evolution in both processing and service in support of process/structure and structure/property modeling for both materials design and development. Through close collaboration of computational engineering companies with tool users we also sought rapid commercially supported dissemination of these new capabilities.

Summary of Technical Accomplishments

The following provides a general summary of overall project technical accomplishments by task, along with a detailed publication list, and example (first pages) from these various publications.

Task 1: Process/Structure Modeling Tools

Microstructure Representation (S. Chan [Northwestern University], H.-J. Jou, J. Sebastian, and Weiming Huang [QuesTek)])

Driven by the need to establish experimental techniques, data processing and quantification of multiscale non-uniform particle microstructure in high performance steels, Northwestern University and QuesTek teamed up to develop innovative approaches. In particular, the focus of this study was placed on grain pinning particles and inclusions, which have significant impact to the fracture toughness and ballistic resistance of materials. A number of collaborative interactions occurred through this portion of the project. For each dataset, the following interactions took place with the noted institutes and people. Examples of the 3D reconstruction techniques, and of the associated 3D particle distribution quantification efforts, follow.

- *Mod4330 and BA160 Crack Tips*
    - NU/NRL (Spanos, Rowenhorst, Everett) – serial sectioning, image processing, X-ray tomography
    - NU/QuesTek (Jou) – 3D reconstruction, primary particle and crack analysis
    - NU (Liu, Tian, Tang) – ductile fracture simulations
    - U. Mich (Pollock, Echlin) – FSL sectioning development
    - Risoe (Lauridsen) – *in situ* Synchrotron XCMT of crack tips (ESRF)
- *C61-La Inclusion Clusters*
    - NRL (Spanos, Rowenhorst) – serial sectioning, particle analysis
    - NU/NRL (Rowenhorst)– image processing, 3D reconstruction
    - GIT (McDowell, Prasannavenkatesan) – fatigue nucleation simulations
    - U. Mich (Pollock, Echlin) – FSL sectioning development
- *Mod4330 Shear Specimen Microvoids*
    - AFRL (Uchic) – FIB/SEM serial sectioning
    - NU/QuesTek (Jou, Sebastian) – image processing, 3D reconstruction, statistical analysis of primary and secondary particles
    - NU (Liu, Tian) – ductile fracture simulations
    - MIT (Parks)– microvoid softening simulations
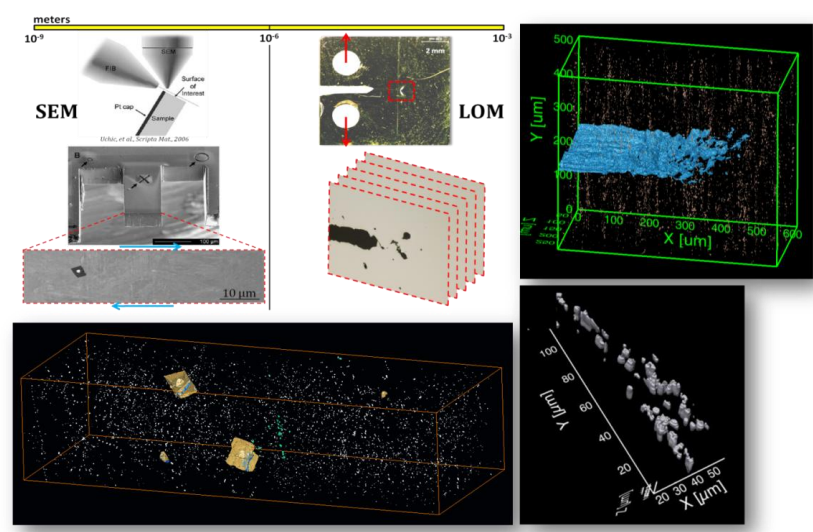
Figure 1: Development of experimental techniques and analysis/visualization tools for SEM and LOM level 3D microstructure, including precipitates, inclusions, hot working damage, microvoids and ductile fracture process

Parameter	Mod4330	BA160
Δa (μm)	91	0 - 100
Process Zone (μm)	186	290
CTOD (μm)	15	65
Critical Void Diameter (μm)	Trans: 37.4 Long: 24.5	Trans: 54.9 Long: 43.9

Mod4330

BA160
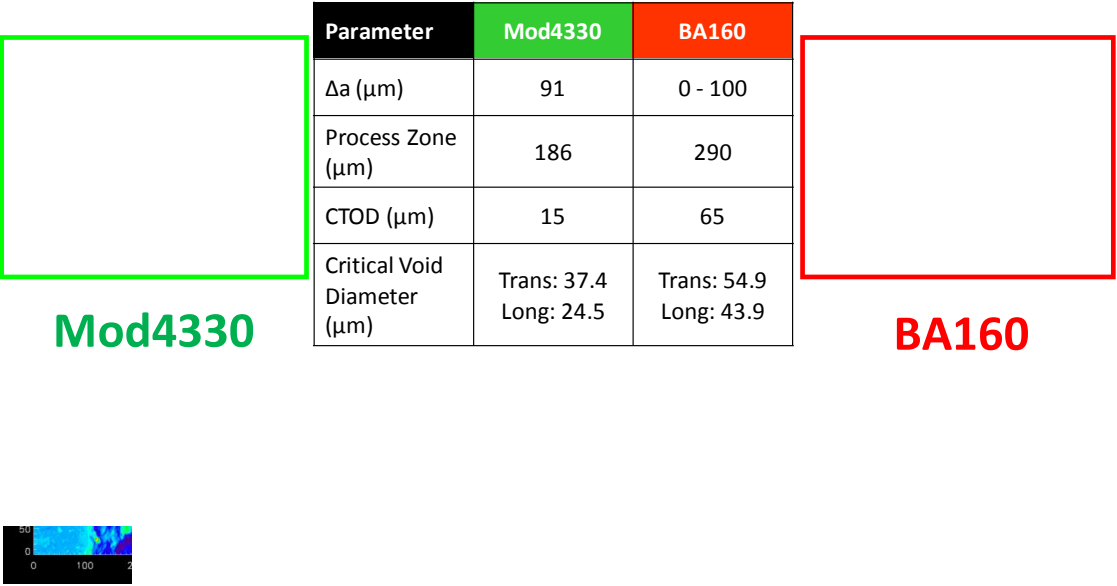
Figure 2: Quantification of ductile fracture microstructure for two steels with different fracture toughness
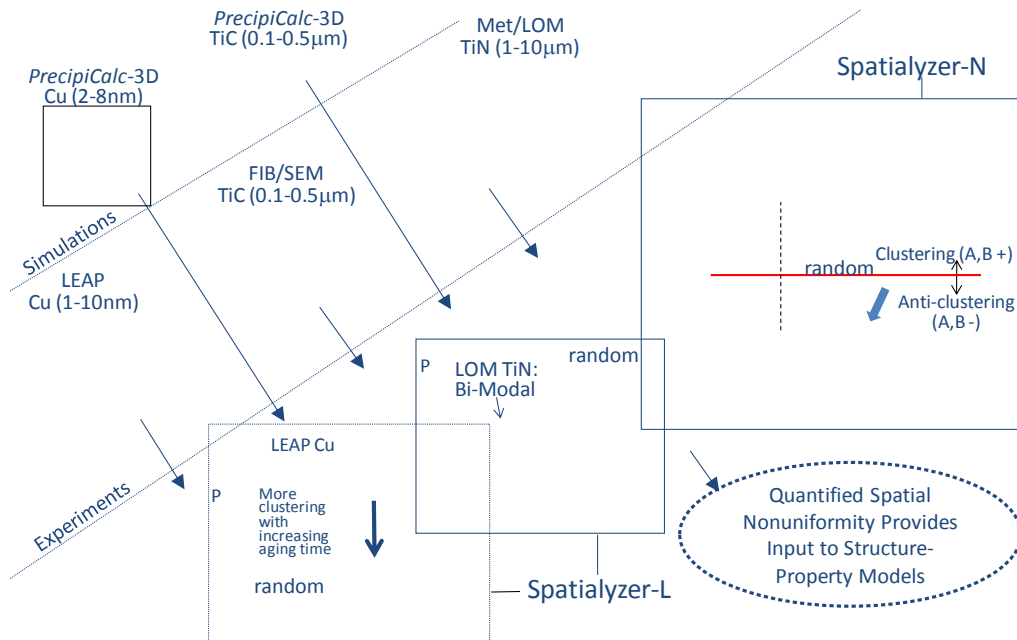
Figure 3: Quantification of precipitate spatial non-uniformity at different length scales in steels

Multiparticle Spatial Interaction (P.W. Voorhees [Northwestern University], H.-J. Jou [QuesTek)])

Driven by the need to model precipitation evolution accounting for the spatial arrangement of precipitates, a multiparticle description of growth and coarsening without the mean field assumption was developed using the multipole method. Development of a new method for efficiently computing particle growth/dissolution and coarsening was also completed.
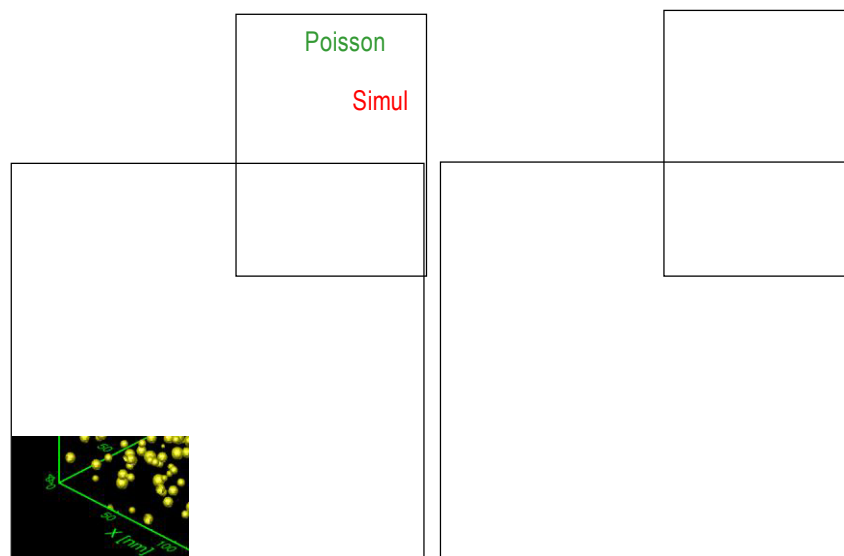
Figure 4: Cu particle coarsening in Fe-Cu aging. Initially spatially uniform (random) distribution moves toward more spatially regular (anti-clustered) arrangement.

Cluster Dynamics Nucleation Model (P.W. Voorhees [Northwestern University], H.-J. Jou [QuesTek)])

Aiming to remove limitations of classical nucleation theory and to explicitly model subcritical cluster formation and evolution, the cluster dynamics nucleation model was investigated. Model implementation in software was also accomplished with input of size-dependent interfacial energy and diffusivity.

Figure 5: Example of cluster/precipitation evolution of an initially supersaturated solid solution. For particles, conventional nucleation/ growth/coarsening behavior is recovered.

Multiparticle Morphological Interaction (P.W. Voorhees, B. Moran [Northwestern University])

To eliminate assumptions regarding particle morphology during precipitation, simulation techniques based on:

- eXtended Finite Element Method (XFEM)—with arbitrary discontinuities in shape functions, no need for re-meshing for interface evolution
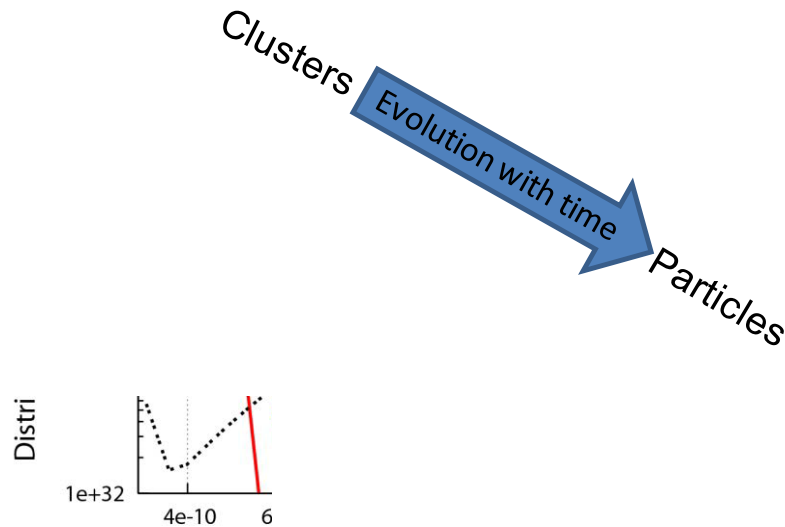- Level Set Method—implicitly tracking of the interface to handle arbitrary interface shape

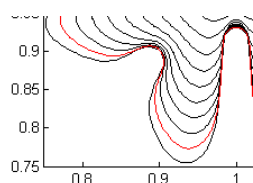were developed in the D3D program.

Figure 6: Simulation examples for evolution of 2D rounded square particle growth in the absence of elastic field (left) and with anisotropic misfit strain (right). The results were validated successfully with available published data.

LEAP 3D Reconstruction of Strengthening Nanostructures (D.N. Seidman and M. Mulholland [Northwestern University])

Experimental technique to quantify microstructure of nanoscale strengthening precipitates in steels was developed. Blastalloy (BA) 160 steel is strengthened by the co-precipitation of copper-rich and M_2C carbide precipitates, where M is a combination of the carbide forming elements Mo, Cr, Ti, and V. Cu and M_2C precipitates are co-located for all aging times characterized. We had assumed that the M_2C carbides are heterogeneously nucleated on the Cu precipitates, but had not observed directly the precipitation sequence. Characterization of BA 160 aged for short times was therefore performed, using local electrode atom probe (LEAP) tomography, to determine the order of precipitation.

- An understanding of the effects of laser-pulsed LEAP tomography on precipitate quantification has been developed. Corrections based on voltage-pulsed data allow the larger datasets produced by laser-pulsed LEAP tomography to be combined with the more accurate quantification provided by voltage-pulsed LEAP tomography.
- Copper and M_2C precipitate average radii, number densities, volume fractions, compositions, and interprecipitate spacings have been measured for a variety of aging treatments. All of this information has been used in the development of an analytical, predictive yield strength model, as well as an understanding of the co-precipitation process.
- Through the complementary use of synchrotron-source XRD, LEAP tomography, and mechanical testing, the origin of the significant toughness increase upon aging BA-160 steel at 550 °C for 30 min and 450 °C for 80 h has been elucidated: the toughness increase is due to dissolution of Fe_3C by precipitation of M_2C carbides. The volume fraction of precipitated austenite present after aging at

550 °C for 30 min and 450 °C for 80 h appears insufficient for transformation induced plasticity to significantly increase the toughness.

(a)   (b)
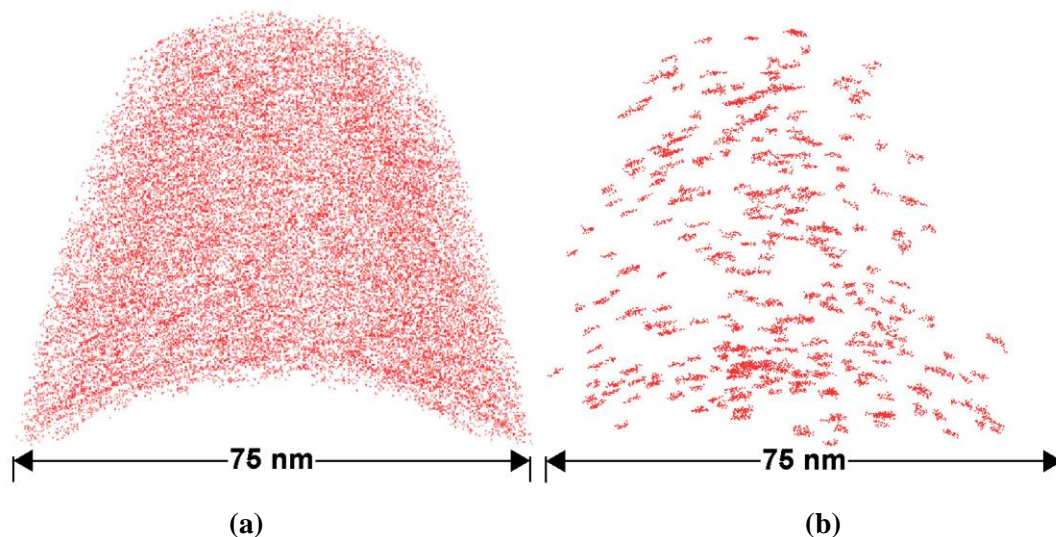
Figure 7: (a) Cu atoms and (b) Cu precipitates in a sample aged for 5 min at 450 °C. Datasets (a) and (b) contain 7 M and 60,000 atoms, respectively.
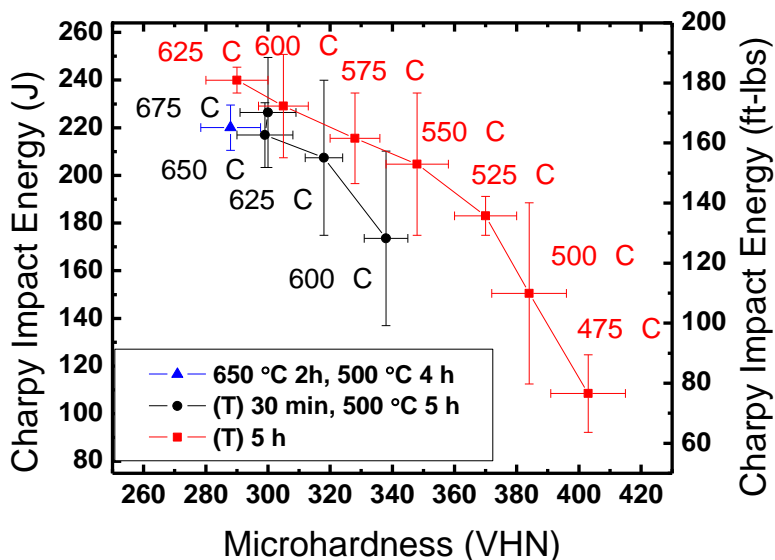
Figure 8: Toughness-microhardness trajectory for samples aged according to protocol (d), samples aged at the aging temperature listed on the graph for 30 min followed by 500 °C for 5 h, and samples subjected to a 5 h isochronal temper. The indicated temperatures next to the isochronally aged samples are the aging temperatures.

Femtosecond Laser (FSL) Tomography 3D Reconstructions of Particle Dispersions (T. Pollock and M. Echlin [University of Michigan])

Aiming to establish a 3D tomographic technique to achieve high sectioning volume to assist identification of extreme microstructrue anomalies, the femtosecond laser 3D tomography was investigated and successfully developed.

- A protocol for layer by layer removal of material by femtosecond laser ablation was developed.
- A fully automated ablation and optical imaging system was developed for acquisition of 3-D datasets.
- Reconstructed datasets of multi-component systems were acquired with the FSLSS technique.
- Datasets measuring approximately 300μm x 300μm x 200μm could be collected in under 48 hours without human supervision of the laser sectional sectioning system beyond initial setup.
- Material removal rates as high as ~7.5 x 10^4 μm^3/s were employed for acquisition of 3-D datasets.
- Preliminary LIBS data fusion protocols have been demonstrated.
- A Tri-Beam system that introduces a femtosecond laser into a focused ion beam system was designed and initial construction was initiated.
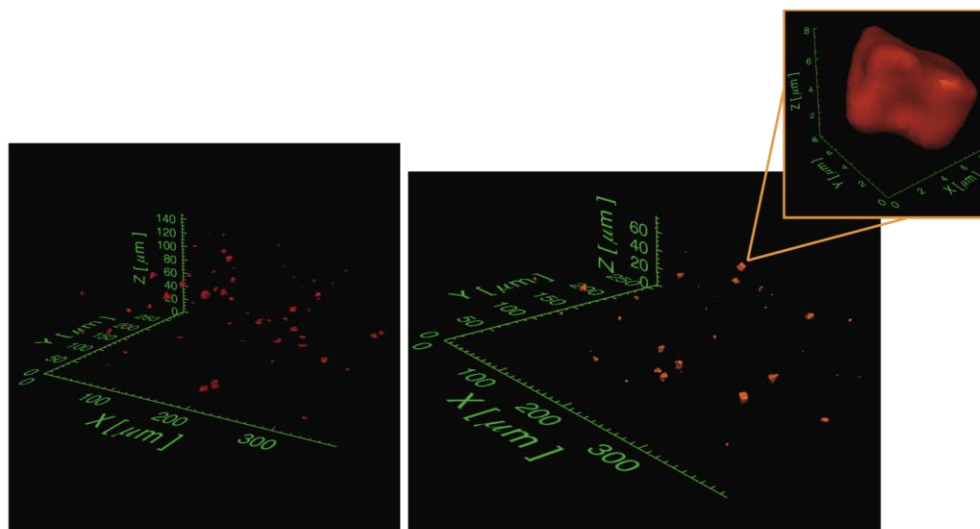
Figure 9: FSLSS 3D dataset of TiN inclusions in titanium modified 4330 steel. (left) image segmentation and reconstruction of datasets from project years 3-4. (right) image segmentation and reconstruction of datasets from project year 5.
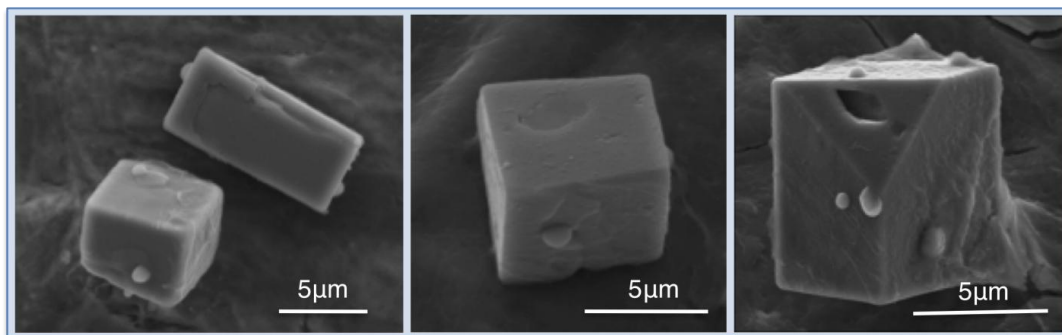

Figure 10: SEM image of TiN particles extracted using a deep etching technique. The cuboidal morphology of the particles is shown in the left two figures. Voids within a nitride are shown in the right image.

Task 2: Structure/Property Modeling Tools

Strength/Toughness Modeling and Simulation (J.S. Wang and H.-J. Jou [QuesTek])

The overall objectives of this subtask were:

- To explore the 3D effects in precipitation strengthening and based on this to develop a 3D yield strength model and a robust tool for the prediction of yield strength from direct 3D measurements of microstructure. Early work focused on analytic modeling of M2C and bcc-Cu precipitation strengthening in ultra-high strength steels and B2 and η-phase strengthening in maraging steels; later work has focused on computer simulations of 3D effects and prediction of yield strength from 3D LEAP data of M_2C and bcc-Cu precipitation in BA160 steel.

- To apply insights from 3D simulation of ductile fracture to develop a model for the prediction of ductile toughness from direct 3D measurements of microstructure and the flow behavior. Early work focused on analyzing literature data of correlations between ductile toughness of steels and the void growth ratio and from these analyses to develop a ductile toughness model; later work has focused on prediction of ductile toughness of the modified 4330 steel from 3D microstructure measurements; and to provide input for more accurate multiscale computational modeling of Mod4330 fracture.
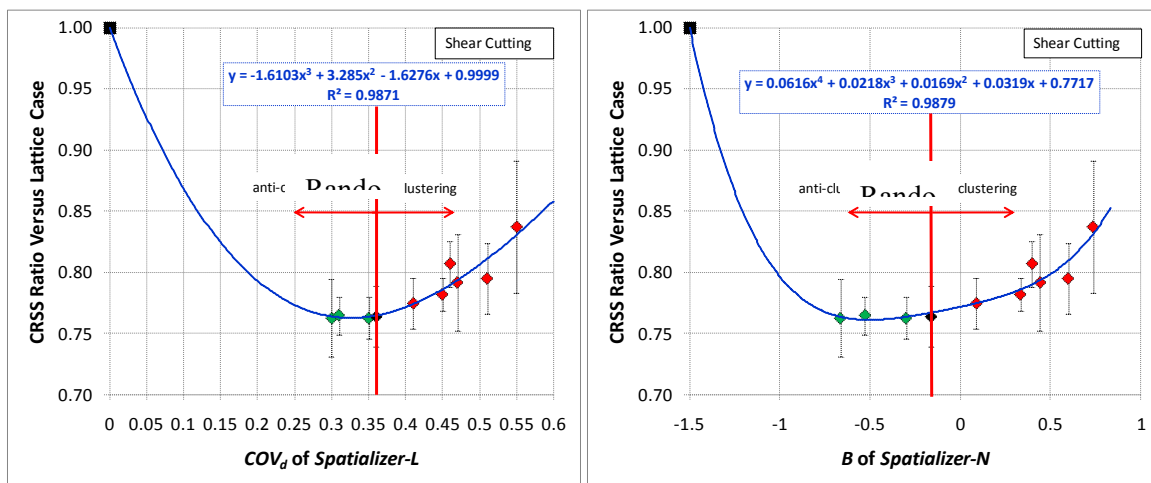
Figure 11: Effect of spatial distribution on CRSS in shear-cutting regime.
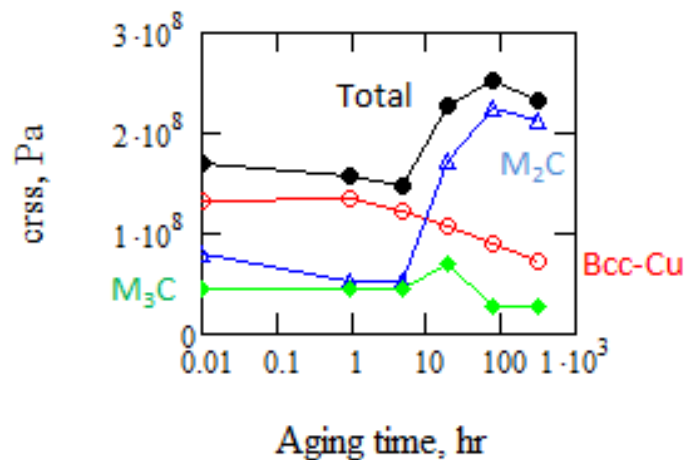
Figure 12: Total precipitation strengthening in BA160 (filled black circles) and contribution from M_2C (blue triangles), bcc-Cu (red circles) and cementite (green filled diamonds)

Multiscale Fracture Simulator (W.K. Liu and B. Moran [NU]; D.M. Parks [MIT])

The overall objective of our project within D3D was the creation and development of simulation tools for fracture of engineering alloys. High toughness steels often have primary and secondary populations of particles. The fracture process is inherently linked to the underlying microstructures of particles. Based on this fracture mechanism and experimental observation, a multiresoltuion model has been developed, which overcomes one of the shortcomings of conventional continuum mechanics. The length scales which can characterize the microstructures (particles) in engineering alloys are naturally introduced into multiresolution model. A modified Gurson model has been developed to take into account the micro-void shear localization mechanism at the length scale of secondary particles and a multiresolution model has been presented, which can consider the deformation across the multiple length scales of microstructures in high toughness alloys. The experimental reconstructed microstructures have been directly embedded in a computational model for fracture prediction.
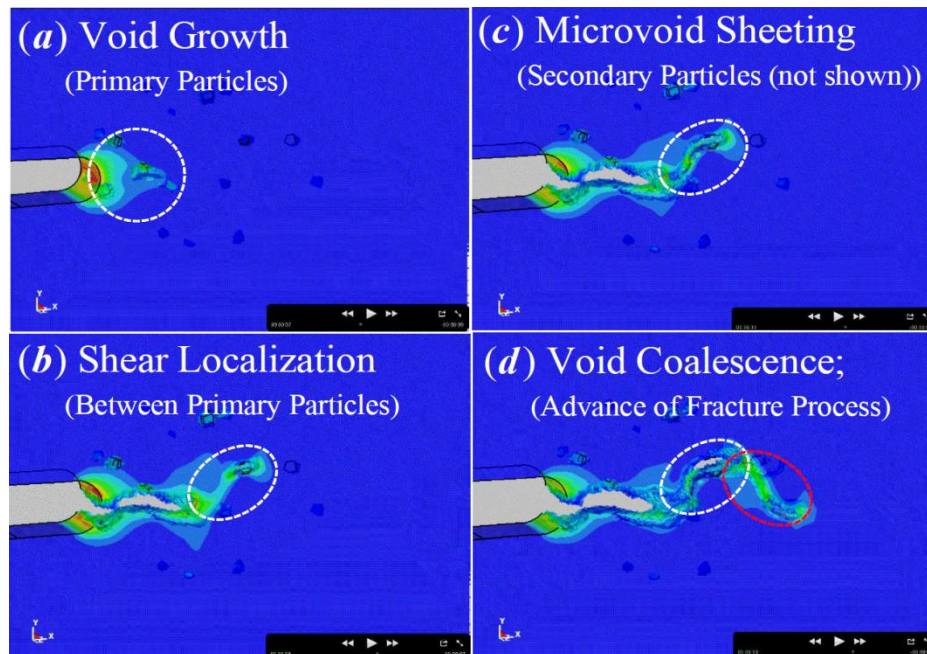
Figure 13: Multiscale shear-driven fracture process

Figure 14: Modified Gurson model describing microvoid shear localization

Multiscale Fatigue Simulator (D. McDowell [GaTech], R. Prasannavenkatesan [QuesTek]])

Key Georgia Tech objectives in the 3D multiscale fatigue simulation effort were directed towards several aspects of 3D constitutive laws and finite element modeling of high cycle fatigue potency of primary inclusions in high strength martensitic gear steels produced by QuesTek, including:

- Development of novel strategies to couple process route (e.g., carburization and shot peening) with microstructure scale response for comprehensive analyses of fatigue potency of critical life-limiting microstructure features in high strength steels.

- Development of relevant constitutive models suitable to investigate the fatigue response at various microstructure scales in martensitic steels.

- Devising schemes for nucleation based minimum life design for debonded inclusions and inclusion clusters.

- Modeling small crack growth at fatigue critical ―hot spots‖.

- Development of multiscale schemes to couple fatigue response at various microstructure scales (collaboration with Prof. W.K. Liu, NU).

- Development of methods for computational study of improved process routes to enhance fatigue resistance.

- Development of probabilistic approaches for extreme value high cycle fatigue variability of lifetime and surface to subsurface transition from LCF/HCF to VHCF regimes.

Figure 15: Challenge statement for hierarchical, multilevel fatigue modeling effort at Georgia Tech, with length scales ranging from sub-micron inclusions and strengthening precipitates to several micron primary inclusions, to subsurface residual stress fields due to shot peening extending several hundred microns into the subsurface. These tools play a key supporting role in tailoring microstructures (including primary forming routes and surface treatment) to maximize fatigue resistance and/or minimize variation.
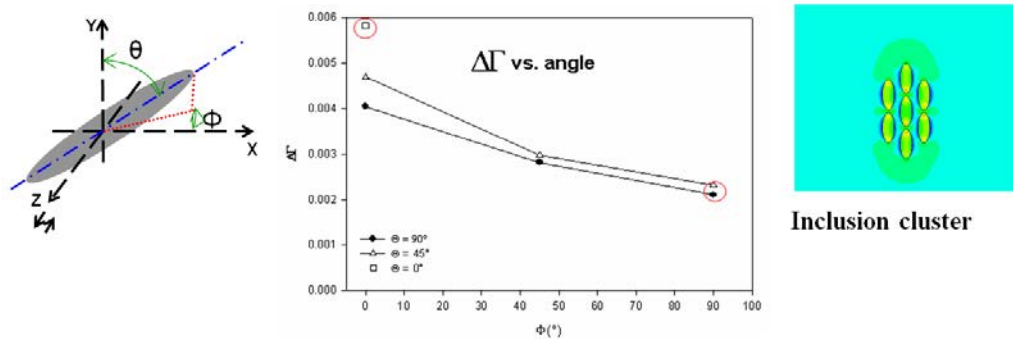
Figure 16: Modeling effects of inclusion orientation on fatigue crack nucleation.
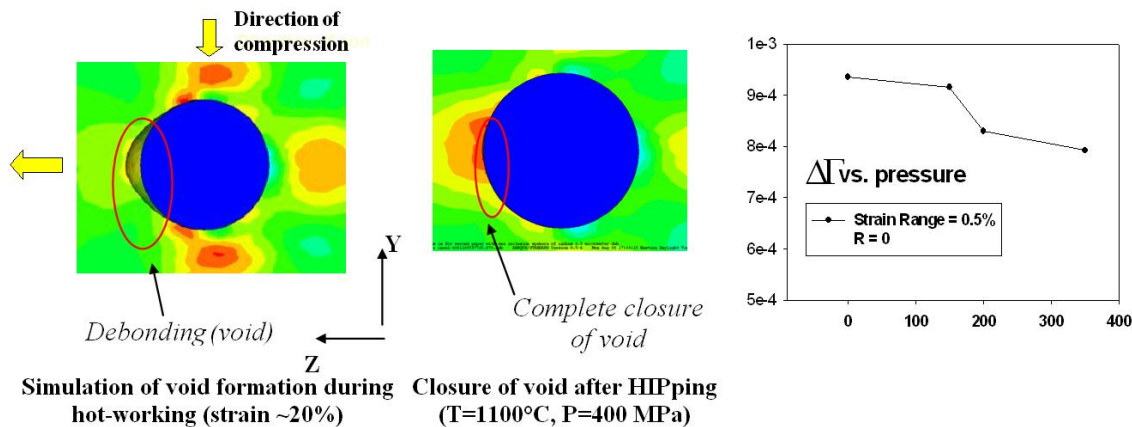
Figure 17: Assessment of Hot Isostatic Pressing (HIPping) on healing of process damage and enhancement of fatigue performance of gear steels.
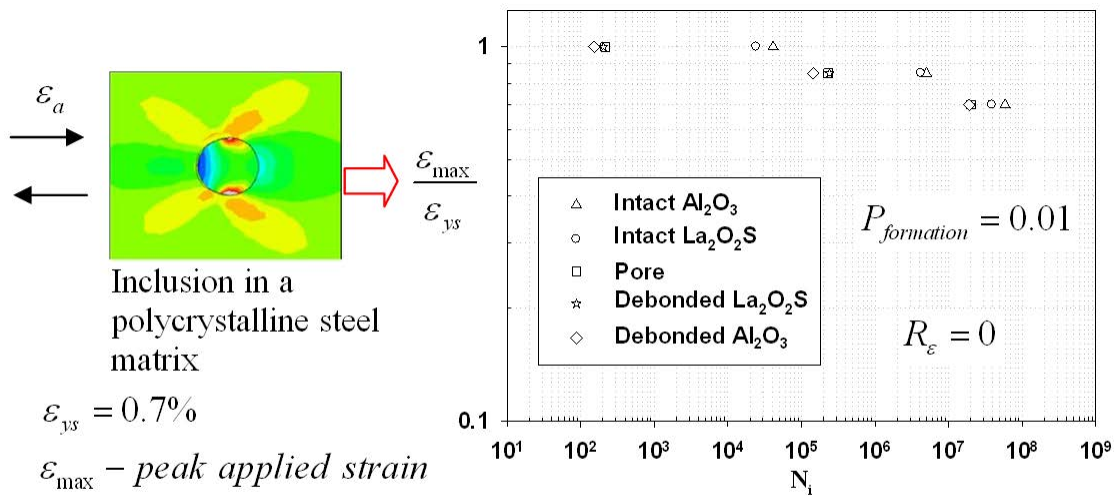
Normalized peak applied strain versus life plot for 1% crack formation probability (minimum life) considering various microstructure attributes

Figure 18: Assessment of extreme value fatigue sensitivity to inclusions and pores in martensitic gear steels.
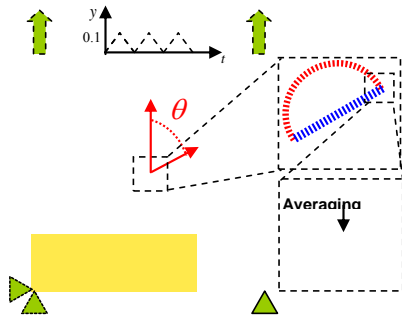
Model geometry, location of the averaging area, and boundary and loading conditions.

Nonlocal FS parameter.

Figure 19: Modeling effects of orientation of inclusion cracking, debonding, and clustering on fatigue crack formation.
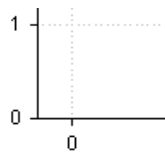
Figure 20: Modeling effects of inclusion interaction in a cluster to discern the effect of shielding arrangements on fatigue potency.

Task 3: Quantum Engineering of Interfacial Properties

Enhanced FLAPW Method and Applications (A.J. Freeman, J. Jerome, and O. Kontsevoi [NU])

Our objective was to accelerate calculations with the precise all-electron full-potential linearized augmented plane wave (FLAPW) method for first-principles density functional calculations to facilitate its application to 3D issues in the adhesion of metal/ceramic interfaces important to the toughness and fatigue strength of high performance alloys. We employed as our application example the interfacial adhesion between an Fe matrix and transition metal carbide/nitride interfaces (M[C,N], where M is a transition metal) of importance to both primary inclusions and secondary grain-refining dispersions in high-strength steels. Our approach centered on phases thermodynamically accessible in steel design, and passed computed adhesive work and force-distance behavior to micromechanics simulations of ductile fracture by Parks at MIT and Liu at NU, while passing detailed computed charge densities to Eberhart at CSM for bond topological analysis.
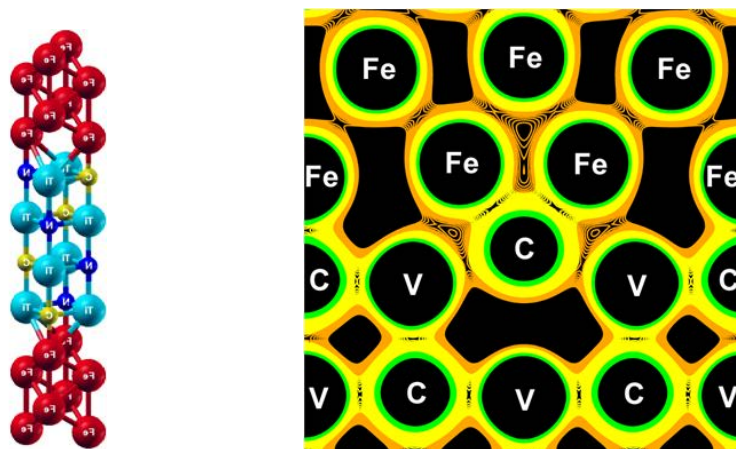
Figure 21: Structure model of Fe/Ti($C_{0.5}N_{0.5}$) interface (left); calculated charge density for semicoherent Fe/VC interface (right).
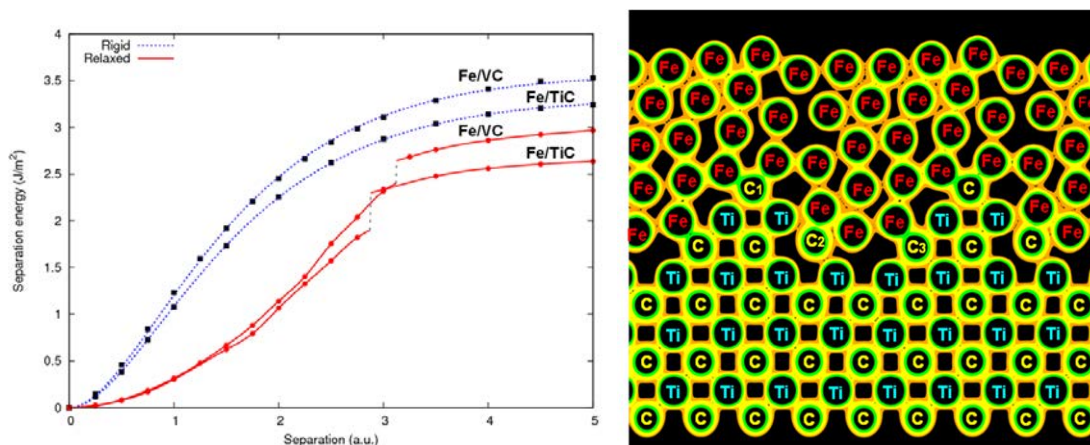
Figure 22: Calculated separation energy vs. separation for semicoherent Fe/VC and Fe/TiC interfaces (left); calculated relaxed bonding charge densities of the stepped Fe/TiC interface (right).
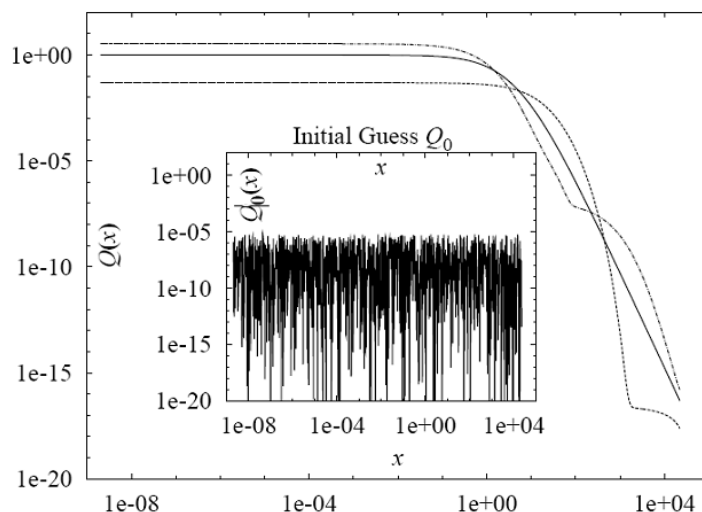
Figure 23: Convergence of the Newton-Raphson algorithm, starting with normalized random numbers. Dashed line: iteration 9, dash-dotted line: iteration 13; solid line: iteration 22. Inset: Random(x).

	Ti	**V**	**Nb**	**Mo**
Ti	3.60	3.58	3.51	3.58
V		3.78	3.66	3.70
Nb			3.69	3.61
Mo				3.58

Figure 24: Calculated work of separation for Fe interface with ternary carbides

Bond Topological Method and Applications (TECD) (M. Eberhart [CSM])

We are concerned with predicting how alloying elements would affect the work of adhesion at an iron-transition metal carbide interface. Specifically, consider the coherent Fe(001)/M1M2C(001) interface, where the M1 and M2 are Ti, V, Nb, or Mo (see Figure 25). Using our software to analyze the charge density determined through direct measurement or as calculated using a quantum mechanical methods (e.g. FLAPW), first neighbor Fe-Fe, Fe-C and M1-C (M2-C) bonds are found, along with Fe-Fe second neighbor bonds. Figure 27 summarizes a strong correlation of adhesive work with the charge density in second-neighbor Fe bonds adjacent to the interface. This leads to the prediction of a beneficial effect of Ni occupancy in this site, with support from recent VASP and FLAPW calculations. This represents a significant validated prediction of bond topological analysis guiding alloy design.
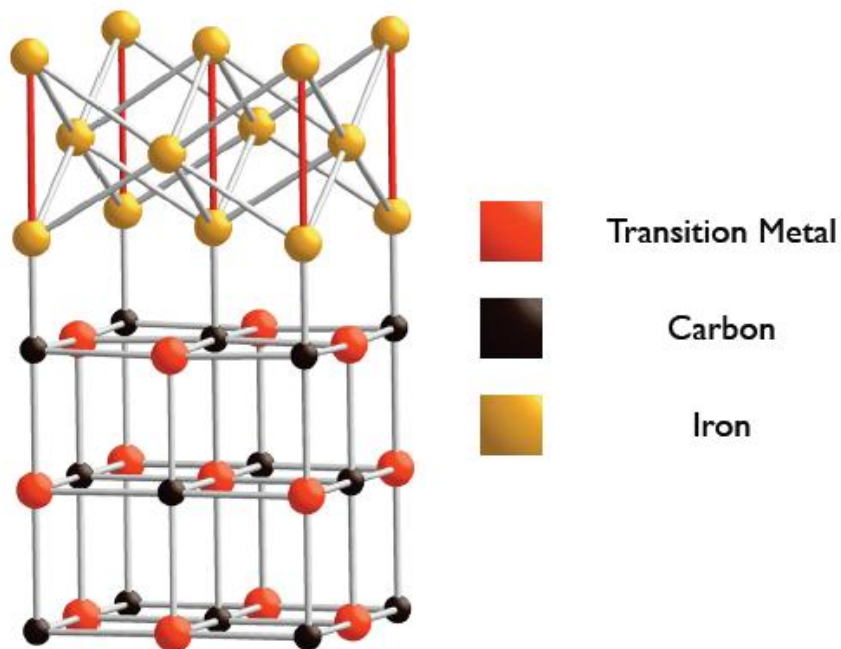
Figure 25: Structure of an iron carbide interface.
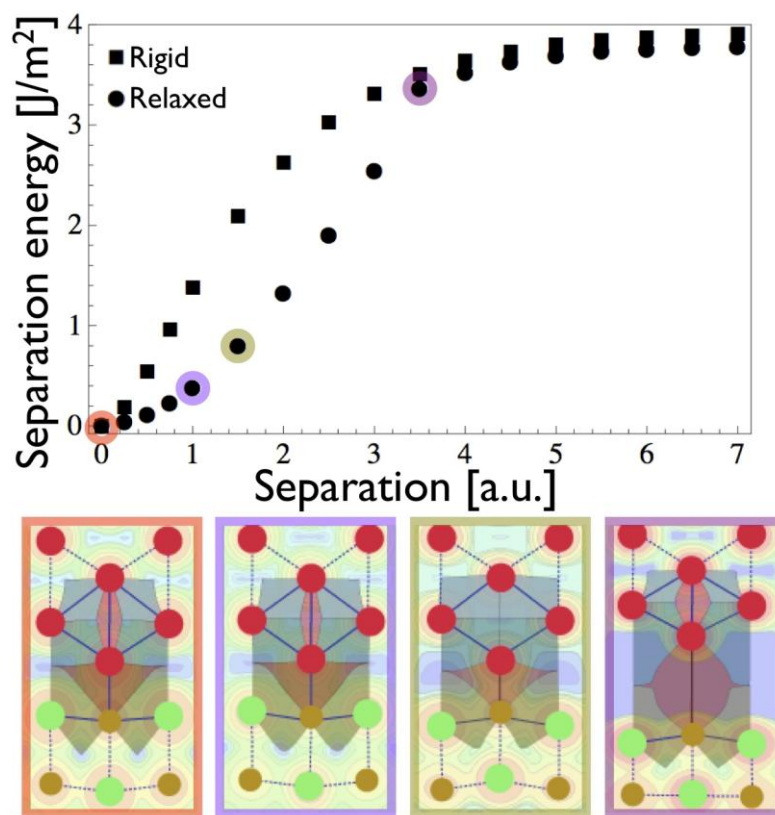
Figure 26: Separation energy (top) and topology (bottom) vs. separation.
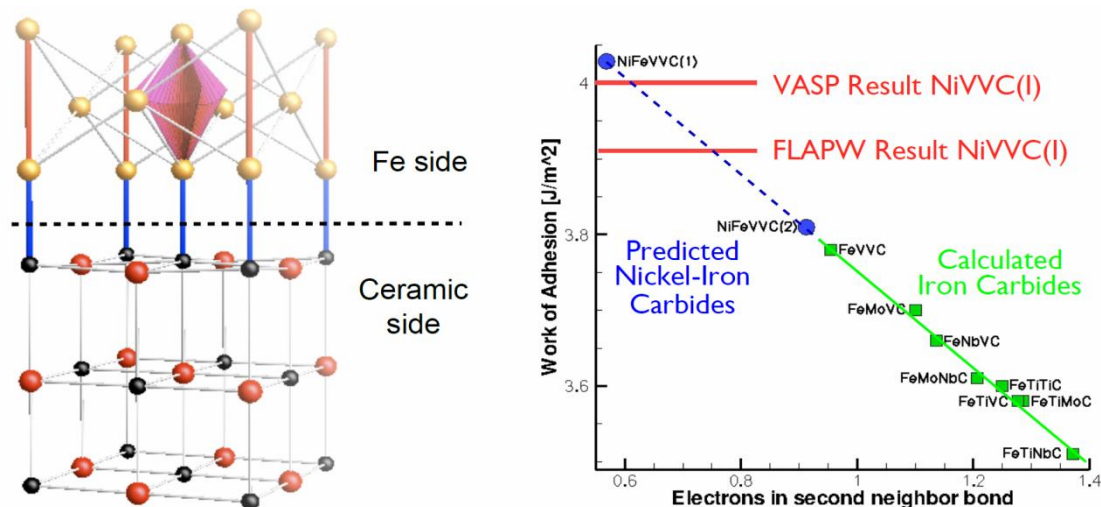
Figure 27: Prediction of a beneficial effect of matrix Ni alloying validated by FLAPW calculations.

Task 4: Use Cases

Use cases motivating purposeful tool development are drawn from separately funded ferrous alloy development programs of consortium participants. A team of materials designers at QuesTek coordinates the focused 3D microstructural characterization experiments of D. Seidman at Northwestern and T. Pollock at University of Michigan with specific applications of the advanced tools of Tasks 1-3. Early applications have been directed at support of development of new Cr-free Ni steels designed by Northwestern and QuesTek in support of a Navy ManTech program. Initial process/structure, structure/property and quantum interfacial modeling center on the optimization of grain refining dispersions (developed during homogenization and hot working treatments) for maximum resistance to microvoid shear localization in air melted steels. Other applications address optimization of precipitation strengthening dispersions (with 3D LEAP validation) and transformation toughening behavior in high strength austenitic steels of interest for nonmagnetic hull and blast protection systems. Discussions with NSWC identified a range of naval ferrous alloy applications in both structures and propulsion systems where application of our microstructure-based fatigue simulation can provide an effective foundation for probabilistic component life modeling. QuesTek and Northwestern also currently collaborate on fundamental fatigue studies of new high performance gear steels relevant to the turbomachinery of both Navy helicopters and next generation Navy fast ships. Such ongoing related experimental fatigue studies provide vital information from well characterized microstructural defects as input into our simulations.

Design integration activities are supplemented by collaboration of graduate research students with undergraduate teams in Prof. Olson's materials design class at Northwestern University. This includes activities of a new senior-level interdisciplinary design course where a continuing project based on current ONR research explores concurrent design of materials and structures for blast protection.

Tool demonstrations initially focused on Ni martensitic steels of naval interest. The Blastalloy160 steel which has been the central focus of detailed LEAP reconstruction of strengthening dispersions is a 6Ni martensitic steel designed as a higher performance version of the Navy's weldable HSLA100 plate steel. It combines bcc Cu and M_2C carbide strengthening with transformation toughening from optimized precipitated austenite to maintain the same impact toughness as HSLA100 out to significantly higher strength levels. Building on results of our shear localization studies, QuesTek designed a 130ksi strength variant of this steel, demonstrating the highest ballistic performance against shear plugging failure in a recent ONR ManTech program for aircraft carrier deck applications. In pursuit of greater improvements in shear localization resistance, precipitation-strengthened austenitic TRIP steels have been designed in a

related ONR-sponsored project at NU; a thorough LEAP study and *PrecipiCalc* simulation of the precipitation strengthening behavior was conducted. Our assessment of strengthening behavior of NiAl and Ni_3Ti phases is motivated by their potential use in Ni maraging steels under consideration for naval aircraft landing gear applications.

As a prototypical Ni martensitic steel, the modified 4330 steel of our earlier ductile fracture studies served as the focus of our FIB/SEM reconstructions of submicron carbides and associated microvoids, as well as our crack tip reconstructions of multiscale fracture. A Ti-modified air-melted steel with numerous multi-micron TiN inclusions, the steel served as a useful test bed for investigation of TiN interfacial damage and particle cracking behavior in shear, and served as a standard material for technique development allowing comparison of conventional metallographic and FSL sectioning.

Our fatigue nucleation studies focused on QuesTek's C61 high-performance M_2C carbide-strengthened gear steel which is demonstrating superior durability in racing applications, while undergoing further development for naval helicopter applications. The observed inclusion clusters motivating our numerical simulations of fatigue nucleation are based on analyzed samples from a previous fatigue testing program. To assist tomographic technique development, a special high-La heat of the steel has been employed to provide higher amounts of La oxysulfide inclusion clusters, again supporting direct comparison of metallographic and FSL sectioning.

Building on our previous experience in computational parametric alloy design and AIM acceleration of development and qualification, our vision of the full cycle of application of the D3D toolset developed here is summarized in Figure 28. Within this framework, the developing tools and D3D research results have been applied over the past 5 years to several Navy sponsored QuesTek SBIR/STTR alloy design projects in various stages of development, as listed in Figure 29:
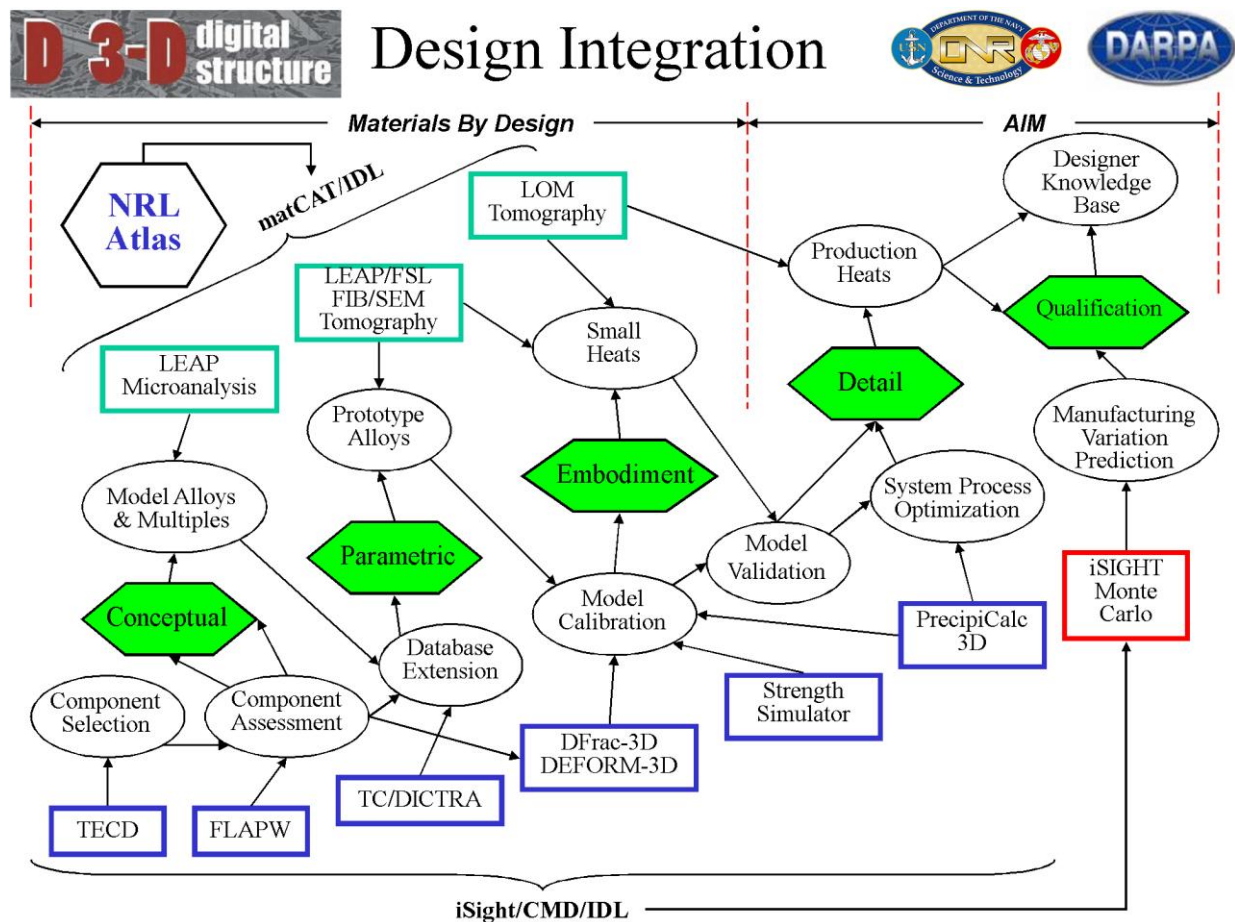
Figure 28: Implementation and integration of D3D toolset for the entire material development cycle.

Figure 29: List of Navy sponsored QuesTek SBIR/STTR projects in the past 5 years.

Funding Agency	Funding Type	Contract Number	Funding Period	Summary
Marine Corps	SBIR Phase II	M67854-05-C-0025	3/17/2005-1/16/2008	High Performance Steel for Expeditionary Fighting Vehicle — Utilization of efficient strengthening precipitates to achieve an unique combination of strength, toughness and corrosion resistance
NAVAIR	SBIR Phase I	N68335-05-C-0207	4/11/2005-6/7/2006	Be-Free High Strength Cu Alloys — Application of precipitation models to alternative strengthening of Cu alloys
NAVAIR	SBIR Phase II	N68335-07-C-0108	12/18/2006-1/8/2009	Be-Free High Strength Cu Alloys — Application of precipitation models to alternative strengthening of Cu alloys
ONR/ NAVAIR	STTR Phase I	ONR: N00014-05-M-0250	8/15/2005-8/31/2006	C64 Gear Steel — Application of fatigue nucleation models to new generation high performance gear steels
ONR/ NAVAIR	STTR Phase II	NAVAIR: N68335-06-C-0339	7/10/2006-7/18/2008	C64 Gear Steel — Application of fatigue nucleation models to new generation high performance gear steels
NAVAIR	SBIR Phase I	N68335-07-C-0302	4/10/2007-8/8/2008	Low Cost High Performance Landing Gear — Application of ductile fracture models to achieve toughness at lower cost
NAVAIR	SBIR Phase II	N68335-08-C-0288	6/30/2008-5/17/2011	Low Cost High Performance Landing Gear — Application of ductile fracture models to achieve toughness at lower cost
ONR	STTR Phase I	N00014-07-M-0445	7/20/2007-2/19/2008	Prognosis Smart Steel — Extension of transformation plasticity models to cyclic conditions for prognosis-enabling state-aware gear steels
NAVAIR	SBIR Phase I	N68335-07-C-0428	9/28/2007-3/31/2008	SCC-Resistance Al Alloy — Extension of strength models to Al systems for designing high strength SCC-resistance Al alloy
ONR/ CTC	ManTech	Non-SBIR Subcontract N00014-00-C-0544	5/01/2005-11/21/2005	Aircraft Carrier Deck Steel — Optimization of grain refining precipitates and shear plugging resistance for optimal ballistic performance
ONR	STTR Phase I	N00014-08-M-0309	6/23/2008-1/19/2009	Integration of Computational Tools for Accelerating Insertion of Aluminum Alloys in Navy Applications
ONR	SBIR Phase I	N00014-09-M-0220	4/16/2009-ongoing	Improved Electrical Contact Materials for Extremely High Current Sliding Contact Materials

NAVAIR	SBIR Phase I	N68335-09-C-0215	4/20/2009-ongoing	Advanced Designs Concepts for High Performance Helicopter Masts
	SBIR Phase II	N68335-11-C-0079	11/1/2010-ongoing	
OSD	SBIR Phase I	N00014-09-M-0400	7/16/2009-ongoing	Innovative Methodologies for the Development of a High Strength, anodize-Free Corrosion Resistant, Aerospace Aluminum Alloys
	SBIR Phase II	TBD	TBD	
NAVAIR	Tailhooks Phase I	N68335-10-C-0174	1/6/10-ongoing	Development of QuesTek alloys for demanding Navy tailhook applications
NAVAIR	EBC Phase I	N68335-10-C-0229	5/11/10-ongoing	Development of innovative new concepts for CMC environmental barrier coatings
NAVAIR	FOD Phase I	N68335-10-C-0421	7/30/10-ongoing	Development of 3-dimensional damage models for CMC foreign object damage
NAVAIR	Spectrum fatigue	N68335-11-C-0055	10/13/10-ongoing	Development of robust fatigue models for spectrum (ultra-high frequency) loading in airframe materials
NAVSEA	SBIR Phase I	N65538-09-M-0088	4/15/2010-ongoing	Development of new materials for use in Navy sacrificial anodes for corrosion protection
	SBIR Phase II	N00024-10-C-4172	10/1/2010-ongoing	
Marine Corps	Phase I	TBD	TBD	Development of SCC-resistant cast aluminum alloys for Marines Corps applications
Marine Corps	Phase I	M67854-10-C-6502	10/23/2009-7/30/2010	Development of Co alloys for Marine Corps machine gun applications

Task 5: Tool Dissemination and Commercialization

Building on the experience of small business collaborations that enabled the successful commercialization of the *PrecipiCalc* code developed under DARPA-AIM, QuesTek worked in parallel with model development to establish a viable plan for broad commercial dissemination of the new tools. W-T Wu of SFTC collaborated with QuesTek on a simplified multiscale fracture simulation implemented within DEFORM-3D in a parallel multiprocessor mode. QuesTek also collaborated with Freeman's company, Quantum Materials Design, to facilitate commercial dissemination of new FLAPW capabilities and quantum-based modeling tools.

DFRAC-3D (W.-S. Wu & A. Bandar [SFTC])

A new commercial tool, DFRAC-3D, has been developed to allow engineers and scientists to observe the effect of varying the morphology of a cluster of pores, as well as varying the value of materials constants in a microvoiding model, on material performance. This tool generates input files for the commercial FEM code DEFORM-3D, to simulate the localized shear and microvoid evolution through a realistic cluster of pre-existing pores in the process zone of a crack tip.

A stand-alone preprocessor for the generation of DEFORM-3D FEM simulation files, called DFRAC-3D (Figure 32), has been developed during the D 3-D program. A library of realistic void distributions, extracted from experimentally observed serial sectioning results provided by D 3-D studies, has been created. These distributions vary the number and total volume fraction of pores within the process zone of a crack tip, so as to provide a range of realistic microstructures with which to simulate realistic fracture. Additionally, the ability to conveniently vary the values of material constants within the microvoiding damage model is integrated into the DFRAC-3D preprocessor. Thus, DFRAC-3D represents a new tool with which to facilitate the investigations of engineers and researchers into the fracture resistance of realistic materials.
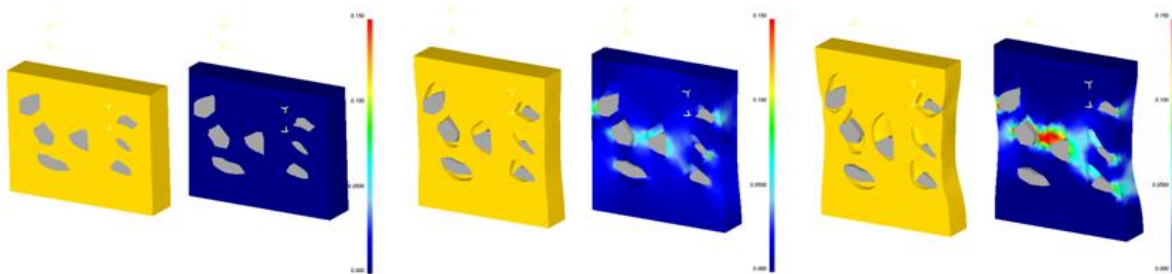
Figure 30: Beginning, middle, and end of tensile deformation of 3D cluster of particles, demonstrating position of particles (yellow workpiece) and strain rate of deforming material (contour plots).
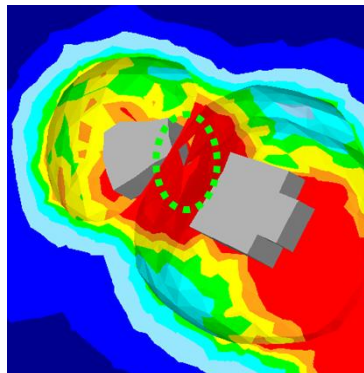
Figure 31: Detail of the initiation of coalescence of voids growing around a pair of particles. (Dotted green line highlights separation of ligament between pores.
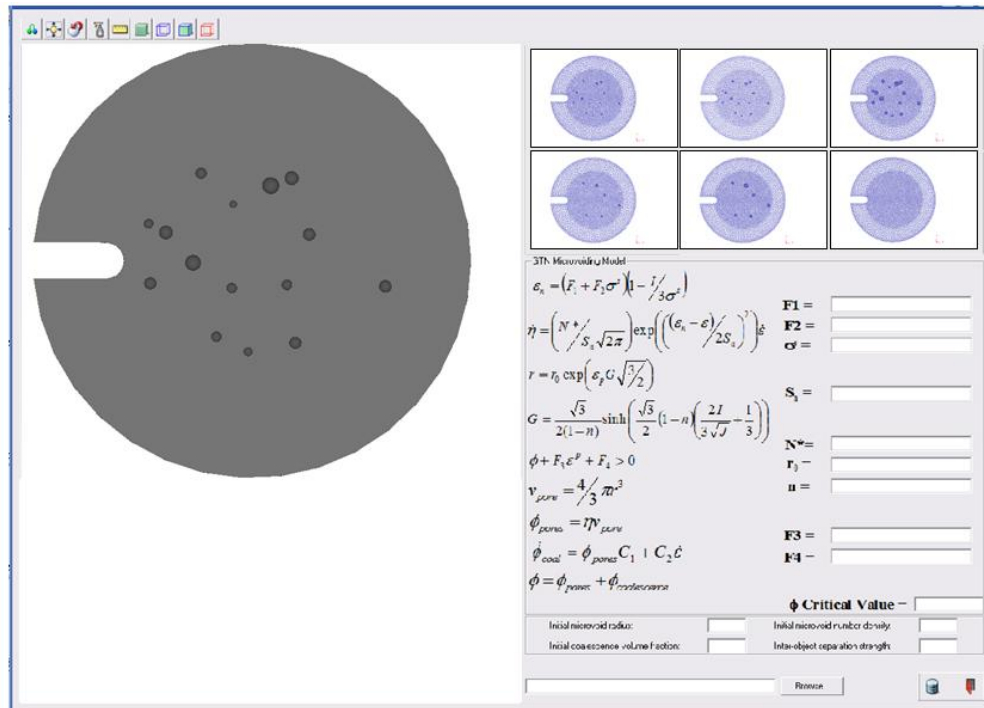
Figure 32: The DFRAC-3D Standalone pre-processor.

Project Deliverables and Publications

Experimental Techniques

- Laser-Assisted LEAP Tomography
    - o Goals:
        - Optimization of operating conditions with 400nm laser
        - Demonstration on BA160 multiphase strengthening dispersion
    - o Dissemination:
        - Instrumentation access available through NUCAPT facility
        - Procedures and applications presented in archival literature publications
            - D.N. Seidman, C.K. Sudbrack, and K.E. Yoon, ―The Use of 3-D Atom-Probe Tomography to Study Nickel-Based Superalloys," JOM, December 2006.
            - R. Karnesky, C.K. Sudbrack and D.N. Seidman, ―Best-fit ellipsoid of atom-probe tomographic data to study coalescence of gamma-prime (L12) precipitates in Ni-Al-Cr", Scripta Mater. 57 (2007) 353-356.
            - R. Karnesky, D. Isheim and D.N. Seidman, ―Direct measurement of two-dimensional and three-dimensional interprecipitate distance distributions from atom-probe tomographic reconstructions," Applied Physics Letters 91, 013111 (2007).
            - M.D. Mulholland and D.N. Seidman, "Multiple dispersed phases in a high-strength low-carbon steel: An atom-probe tomographic and synchrotron X-ray diffraction study," Scripta Materialia 2009;60:992.
            - M.D. Mulholland and D.N. Seidman, "Nanoscale co-precipitation and mechanical properties in a high strength, low carbon steel," Acta Materialia. 2010, in press
            - M.D. Mulholland and D.N. Seidman, "The effects of laser-pulsed atom probe tomography on precipitate analysis in a high strength low carbon steel," submitted to Microscopy. and Microanalysis. 2010
        - Tomographic reconstructions of multiphase particle dispersions in BA160 disseminated through D3D website.
- LOM and FIB/SEM Tomography
    - o Goals:
        - Optimized laser-ablative serial sectioning techniques for large RVE datasets
        - Demonstration and comparison with other techniques for primary inclusion clusters in mod4330 (TiN) and C61-La (La2O2S)
    - o Dissemination:
        - Facility access on contract basis
        - Techniques and applications in archival literature
            - M. Echlin, J. Nees, N. Husseni and T.M. Pollock, ―ANew Femtosecond Laser-Based Tomography Technique for Multiphase Materials", Advanced Materials, under review, (2010).

- M. Echlin, N. Husseni and T.M. Pollock, "Clustering of TiN Particles in Steel: A New Tomography Approach", Acta Materialia, under preparation.
- M. Echlin, J. Nees, N. Husseni and T.M. Pollock, "Layer by Layer Femtosecond Laser Ablation for Development of 3-D Datasets", Journal of Applied Physics, under preparation.
- M. Echlin and T.M. Pollock, "Imaging with Laser-Induced Breakdown Spectroscopy and Femtosecond Laser Serial Sections", Scripta Materialia, under preparation.
- M. Echlin, A. Mottura and T.M. Pollock, "A Tri-Beam System for Acquisition of High Resolution 3-D Datasets", Microscopy and Microanalysis, under preparation.
- Reconstructed datasets distributed through D3D website Materials Atlas Database (VTK file formats, Paraview readable)
  - Mod4330 Steels Shear Bar Center Microstructure Showing Microvoids and Various Microstructure Features, including:
    - Presentations detailing experimental procedure (Uchic/AFRL) and key results
    - Processed 2D sectioning images for different microstructure features: TiC, TiN with fracture, microvoid and oxide
    - Amira input file to visualize microstructure in 3D
    - Two 3D image sequences output from Amira

Tomographic Data Analysis

- Particle Spatial Distribution Representation
  - Goals:
    - Quantification of spatial nonuniformity (density, spacing)
    - Demonstration on multiple length scales (nanoscale strengtheners, submicron grain-refiners, multi-micron inclusions)
  - Dissemination:
    - Techniques and applications in archival literature
      - J.S. Wang and H.-J. Jou, "The 3D effects in Nano-Particle Strengthening," in preparation
    - "Spatialyzer-N" and "Spatialyzer-L" codes distributed through D3D website, including:
      - Summary and presentation documentation of background and key results
      - Source codes in IDL and python provided
      - Input data sets from experiments and simulations
- Strength Models
  - Goals:
    - New analytical strength models using tomographic information and dislocation simulation
    - Demonstration on Cu+M2C in BA160
  - Dissemination:
    - Archival literature publication

- J.S. Wang and H.-J. Jou, "The 3D effects in Nano-Particle Strengthening," in preparation
- J.S. Wang, M. D. Mulholland and D. N. Seidman, "Yield Strength Prediction of a Blast Alloy," in preparation
- J.S. Wang and G.B. Olson, "Mechanism of Bcc-Cu Particle Strengthening in Steels," in preparation
- J.S. Wang and G.B. Olson, "M2C Precipitation Strengthening in Steels," to be submitted

- Toughness Models
  - Goals:
    - New analytical ductile toughness model based on tomographic input to multiscale simulation
    - Demonstration on mod4330, BA160 and literature data
  - Dissemination:
    - Archival literature publication
      - J.-S. Wang and G. B. Olson, ―Prediction of ductile fracture toughness‖, Int. Conf. Fracture, Ottawa, Canada, July 13-17, 2009.

3D Simulators

- "PrecipiCalc-3D" Precipitation Simulator
  - Goals:
    - Incorporation of 3D diffusion field interaction via multipole method
    - Demonstration on Cu and TiC evolution (with tomographic input)
    - Incorporation of cluster dynamics nucleation model
    - Demonstration on austenitic TRIP120 (with tomographic input)
  - Dissemination:
    - Archival literature application examples
      - Paper in preparation by Farjami and Voorhees
    - Commercial code distribution and maintenance by QuesTek
    - Simulation examples on D3D website
- Multiscale Fracture & Fatigue Research Simulators
  - Goals:
    - Multiscale simulation of fracture with tomographic input
    - Demonstration on mod4340, BA160 fracture
    - Collaboration with QuesTek and GIT
  - Dissemination:
    - Archival literature application examples
      - C. McVeigh, W. K. Liu, "Prediction of Central Bursting during Axisymmetric Cold Extrusion of a Metal Alloy containing Particles," International Journal of Solids and Structures, 43:10, 3087-3105, 2006.
      - F. Vernerey, C. McVeigh, W. K. Liu, B. Moran, D. Tewari, "3D Computational Modeling of Shear Dominated Ductile Failure of Steel," Journal of Minerals, 58:12, 45-51, 2006.

- C. McVeigh, F.Vernerey, W. K. Liu and C. Brinson, "Multiresolution Analysis for Material Design," Computer Methods in Applied Mechanics and Engineering, 95:37-40, 5053-5076, 2006.

- C. McVeigh, F. Vernerey, W. K. Liu, B. Moran, "An Interactive Microvoid Shear Localization Mechanism in High Strength Steels," Journal for the Mechanics and Physics of Solids, 55:2, 225-244, 2007

- F. Vernerey, W. K. Liu and B. Moran, "Multiscale Micromorphic Theory for Hierarchical Materials," Journal of the Mechanics and Physics of Solids, Volume 55, Issue 12, Pages 2603-2651, December 2007.

- F. J. Vernerey, W. K. Liu, B. Moran, G.B. Olson, "A Micromorphic Model for the Multiple Scale Failure of Heterogeneous Materials," Journal of the Mechanics and Physics of solids, 56(4), 1320-1347, 2008.

- X. Yin, W. Chen, A. To, C. McVeigh, W. K. Liu, "Statistical volume element method for predicting microstructure–constitutive property relations," Comput. Methods Appl. Mech. Engrg. 197 (2008) 3516–3529

- C. McVeigh, W. K. Liu, "Linking microstructure and properties through a predictive multiresolution continuum," Comput. Methods Appl. Mech. Engrg. 197 (2008) 3268–3290.

- W. K. Liu and C. McVeigh, "Predictive Multiscale Theory for Design of Heterogeneous Materials," Computational Mechanics, 42(2), 147-170, 2008.

- C. McVeigh and W. K. Liu, "Multiresolution modeling of ductile reinforced brittle composites," J. Mech. Phys. Solids, 57 (2009) 244–267.

- W. K. Liu, L. Siad, R. Tian, S. Lee, D. Lee, X. Yin, W. Chen, S. Chan, G. B. Olson, L.-E. Lindgen, M. F. Horstemeyer, Y.-S. Chang, J.-B. Choi and Y. J. Kim, "Complexity science of multiscale materials via stochastic computations," International Journal for Numerical Methods in Engineering, Volume 80, Issue 6, 5 - 12 November 2009, Pages: 932-978, 2009.

- F. Vernerey, W. K. Liu, B. Moran, and G. B. Olson, "Multi-length scale micromorphic process zone model," Computational mechanics, Volume 44 (3), August 2009, pp. 433-445.

- W. K. Liu, D. Qian, S. Gonella, S. Li W. Chen, S. Chirputkar, "Multiscale Methods for Mechanical Science of Complex Materials: Bridging from Quantum to Stochastic Multiresolution Continuum," to appear in Int. J. Numer. Meth. Engng (2010).

- C. McVeigh and W. K. Liu, "Multiresolution Continuum Modeling of Micro-void Assisted Dynamic Adiabatic Shear Band Propagation," J. Mech. Phys. Solids, Volume 58, Issue 2, February 2010, Pages 187-205.

- F. Vernerey, PhD Dissertation "Multi-Scale Continuum Theory for Microstructured Materials", May 2006, Northwestern University

- C. McVeigh, PhD Dissertation "Linking Properties to Microstructure through Multiresolution Mechanics", Dec 2007, Northwestern University.

- F. Vernerey, C. McVeigh, W. K. Liu, and B. Moran, "Multiscale Continuum Theory for Heterogeneous Materials," Book Chapter in COMPLAS VIII, E. Onate and R. Owen (Editors), by Springer, 2007.

- F. Vernerey, C. McVeigh, W. K. Liu, B. Moran, D. Tewari, D. Parks, G.B. Olson, ―3D Computational Modeling of Shear Dominated Ductile Failure of Steel,'' JOM, December 2006.
- R. Tian, S. Chan, S.Tang, A.M. Kopacz, J.-S. Wang, H.-J. Jou, L. Siad, L.-E. Lindgren, G.B. Olson, W. K. Liu, "A multiresolution continuum simulation of the ductile fracture process" J. Mech. Phys. Solids. Volume 58, issue 10, 1681-1700.
- S. Tang, A. Kopacz, S. Chan, G.B. Olson, W.K. Liu, "Implementation of three dimensional multiresolution theory into LS-DYNA: formulation and algorithmic aspects" In preparation.
- R. Prasannavenkatesan, PhD dissertation "Microstructure-Sensitive Fatigue Modeling of Heat Treated and Shot Peened Martensitic Gear Steels", December 2009, Georgia Institute of Technology.
- J. Zhang, R. Prasannavenkatesan, M.M. Shenoy, and D.L. McDowell, ―Modeling fatigue crack nucleation at primary inclusions in carburized and shot-peened martensitic steel," Engineering Fracture Mechanics, 76, 2009, pp 315-334.
- R. Prasannavenkatesan, J. Zhang, D.L. McDowell, G.B. Olson, and H.-J. Jou, ―3D modeling of subsurface fatigue crack nucleation potency of primary inclusions in heat treated and shot peened martensitic gear steels," International Journal of Fatigue, 2009, 31, pp 1176-1189.
- R. Prasannavenkatesan, D.L. McDowell, G.B. Olson, and H.-J. Jou, ―Modeling effects of compliant coatings on HCF resistance of primary inclusions in high strength steels," Journal of Engineering Materials and Technology, 2009, 131, pp 011012-011016.
- R. Prasannavenkatesan, C. P. Pryzbyla, N. Salajegheh, D.L. McDowell, "Simulated Extreme Value Fatigue Sensitivity to Inclusions and Pores in Martensitic Gear Steels," submitted to Engineering Fracture Mechanics, 2010.
- C. Przybyla, R. Prasannavenkatesan , N. Salajegheh, and D.L. McDowell, ―Microstructure-Sensitive Modeling of High Cycle Fatigue," International Journal of Fatigue, 2008 (in print).
- R. Prasannavenkatesan, D.L. McDowell, ―Polycrystal plasticity modeling of residual stress relaxation in shot peened martensitic gear steels," Journal of Engineering Materials and Technology, 2010 (accepted and in print).
- Distribution of routines and UMATs (ABAQUS based), C++ paralleled code, LS_DYNA based USER ELEMENT through D3D website
- Simulations and companion crack tip tomographic reconstructions posted to D3D website
- DEFORM-3D "DFrac" Toughness Design Simulator
  - Goals:
    - Reproduce primary functionality of research fracture simulator in robust user-friendly commercial package
    - Demonstration on mod4330
  - Dissemination:
    - Archival literature application example

- ▪ Commercial "D3D-DFrac" package for distribution and maintenance with DEFORM-3D by SFTC
- ▪ Incorporation into UG materials design curriculum at NU
- ▪ Application example on D3D website
- FLAPW Interfacial Quantum Engineering Tool
    - o Goals:
        - ▪ Accelerated FLAPW code capability for prediction of IPB adhesion
        - ▪ Demonstration on MX/Fe coherent and semicoherent interfaces
    - o Dissemination:
        - ▪ Archival literature publications
            - J.W. Jerome, P.R. Sievert, L.-H. Ye, I.G. Kim and A.J. Freeman, ―Convergence of density functional iterative procedures with a Newton-Raphson algorithm", J. Comput. Electron (2007) 6:349-352.
            - J.-H. Lee, T. Shishidou, Y.-J. Zao, A.J. Freeman, G.B. Olson, "Strong interface adhesion in Fe/TiC," Philosophical Magazine, V.85, N.31, pp.3683-3697 (2005)
            - B. Chini, J.W. Jerome, and R. Sacco, ―Multi-physics modeling and finite element approximation of charge flow in ionic channels," Proceedings of Eurosime 2006, IEEE Shaker Publishing, pp. 153-160.
            - M. Longaretti, G. Marino, B. Chini, J.W. Jerome, and R. Sacco, ―Computational models in nano-bio-electronics: simulation of ionic transport in voltage operated channels," Journal of Nanoscience and Nanotechnology 8 (2008), 3686-3694.
            - M. Longaretti, B. Chini, J.W. Jerome, and R. Sacco, ―Electrochemical modeling and characterization of voltage operated channels in nano-bio-electronics," Sensor Letters 6 (2008), 49-56.
            - M. Longaretti, B. Chini, J.W. Jerome, and R. Sacco, ―Computational modeling and simulation of complex systems in bio-electronics," Journal of Computational Electronics 7 (2008), 10-13.
            - C. de Falco, J. Jerome, and R. Sacco, "Quantum corrected drift-diffusion models," Journal of Computational Physics, 228 (2009), 1770-1789.
        - ▪ Commercial "D3D-IPB" slab model package for distribution and maintenance by Quantum Materials Design
        - ▪ Application examples (3D charge distributions) on D3D website
            - Semicoherent Fe/TiC interface fracture - FLAPW 3D charge density results and visualization versus separation distances, including:
                - o FLAPW first principle calculation results and corresponding presentation file
                - o Postprocessing code and results to enable Amira 3D visualization of charge density
                - o Resulting 3D charge density images at varying separation distances
- Bond Topological Analysis Tool
    - o Goals:

- ▪ Efficient bond topological analysis of 3D charge densities from DFT (FLAPW) computations
- ▪ Demonstration of bond topological structure/property relations for MX/Fe adhesion
  - o Dissemination:
    - ▪ Archival literature publications
      - • T.E. Jones and M.E. Eberhart, "Topology of the Charge Density in Ru and Zr," ACTA Crystal A. 65, 141-144, 2009.
      - • T.E. Jones and M.E. Eberhart, "The Bond Bundle in Open Systems," International Journal of Quantum Chemistry, on line publication 13 Oct 2009.
      - • T.E. Jones, and M.E. Eberhart, "The Irreducible Bundle: Further Structure in the Kinetic Energy Distribution," Journal of Chemical Physics, 130, 204108 2009
      - • T.E. Jones, M. Sauer, and M.E. Eberhart, "First Principles Study of Mode I Fracture of Fe/TiX Interfaces (X = C, N)," Physical Review B, 78, 092104 2008.
      - • T.E. Jones, M.E. Jones, and D.P. Clougherty, "Topology of the Spin-polarized Charge Density in bcc and fcc Iron," Physical Review Letters, 100, 017208, 2008.
      - • T.E. Jones, M.E. Eberhart, D.P. Clougherty and C. Woodward, "Electronic Selection Rules Controlling Dislocation Glide in BCC Metals," Physical Review Letters, 101, 085505, 2008
      - • M.E. Eberhart, T.E. Jones, and M. Sauer, "Visualizing the Metallic Bond," Journal of Metals, 60, 67-72, 2008.
      - • M.E. Eberhart, T.E. Jones and D.P. Clougherty, "A Jahn-Teller Model for Metallic Glass Structure and Stability," in preparation
      - • T.E. Jones, M.E. Eberhart and D.P. Clougherty, "Indicators for Topological Phase Transitions Within the Total Charge Density," in preparation
    - ▪ TECD "Bondalyzer" tool distributed and maintained by TecPlot
    - ▪ 3D topological analysis of FLAPW output examples posted to D3D website

Integrated Computational Materials Design Services

- • Goals:
  - o Integration of use-driven D3D tools in Materials Design/AIM methodology
  - o Demonstration in DoD materials design/development projects
- • Dissemination:
  - o Full D3D toolset available for contract design at QuesTek

Design Integration
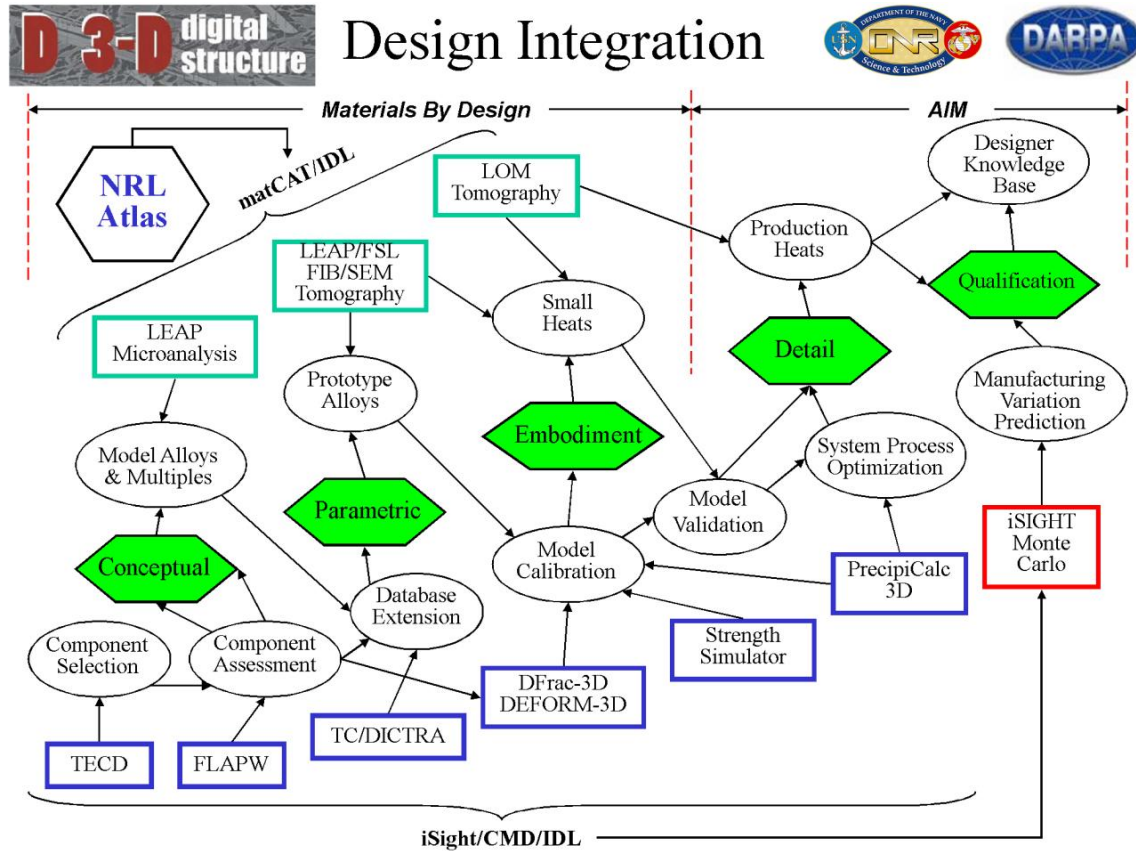
Program Statistics

Graduate students supported (with at least 25% support):

- Franck Vernerey, Ph.D. in 2006 from Northwestern University, currently Assistant Professor at University of Colorado Boulder.
- Cahal McVeigh, Ph.D. in 2007 from Northwestern University, currently at Exponent Inc, Menlo Park, CA.
- Rajesh Prasannavenkatesan, Ph.D. in November, 2009 from Georgia Institute of Technology, currently Materials Design Engineer at QuesTek
- Nicholas Hatcher, Ph.D. in 2009 from Northwestern University, currently Postdoctoral Fellow at Interdisciplinary Centre for Advanced Materials Simulation, Germany
- Mike Mulholland, Ph.D. in June, 2010 from Northwestern University, currently at ArcelorMittal
- Stephanie Chen, Ph.D. candidate, Northwestern University
- Nima Salajegheh, Ph.D. candidate, Georgia Institute of Technology
- Deepti Tewari, Ph.D. candidate, Massachusetts Institute of Technology
- McLean Echlin, Ph.D. candidate, University of Michigan
- Travis Jones, Ph.D. candidate, Colorado School of Mines

Postdoctoral Fellows supported:

- Rong Tian, Northwestern University, 2005-2009
- Oleg Kontsevoi, Northwestern University, 2005-2010
- Susan Farjami, Northwestern University, 2006-2008
- Shan Tang, Northwestern University, 2009-2010
- Dennis Zheng, Northwestern University, 2009-2010

Example Publications

The following appendix includes the first pages of some 25+ select publications (reprints or pre-prints submitted for publication) that are a direct product of the research efforts of QuesTek's DARPA / ONR D3D program. This is only a small selection of the total number of publications, presentations, theses, etc. resulting from the program (see the previous section of this final summary report).

The Use of 3-D Atom-Probe Tomography to Study Nickel-Based Superalloys

David N. Seidman, Chantal K. Sudbrack, and Kevin E. Yoon

Enhanced for the Web

Read this article on the *JOM* web site (*www.tms.org/JOMPT*) to see a video clip of detected γ' precipitate coagulation and coalescence.

Editor's Note: Alloy compositions are given in atomic percent.

Recent technological advances in the design and fabrication of atom-probe tomographs and their commercialization are revolutionizing our ability to determine, on a sub-nanometer scale (atomic scale), the chemical identities of atoms in a nanostructure and to reconstruct this information in three dimensions. Thus, it is now possible to obtain data sets containing several hundred million atoms in a few hours, using either electrical or laser (femtosecond or picosecond) pulsing, and to reconstruct crystalline lattices using sophisticated software programs. Detailed quantitative

results of the application of atom-probe tomography to study the kinetic pathways for precipitation in model nickel-based superalloys, Ni-Al-Cr and Ni-Al-Cr-Re, are presented as illustrative examples.

INTRODUCTION

Atom-probe tomography (APT) is revolutionizing the ability to characterize materials at the sub-nanometer scale (atomic scale) and to obtain three-dimensional (3-D) microstructural information that is germane for understanding both physical and mechanical properties of materials, thereby fulfilling the microstructure-property relationship that is a basic paradigm of materials science and engineering. Recent advances in APT permit the analysis of metals, semiconductors, oxides, and organic materials, albeit with different degrees of success and ease. This is due to a number of important technological advances that have resulted in sophisticated com-

mercial instruments that are computer controlled, ergonomic, and employ sophisticated software for analyzing the large data files, $>10^8$ atoms, which are now possible to obtain.

Atom-probe tomography is being utilized by researchers around the world to study different physical problems utilizing commercial instruments (Cameca, of Gennevilliers, France, or Imago Scientific Instruments of Madison, Wisconsin). The results of a fraction of this research can be found in the biennial *Proceedings of the International Field Symposium*[1] and in the general archival literature. See the sidebar, The Instrument, for a description of an APT, and the sidebar, LEAP™ Tomography, for a discussion on the characterization of nanostructures in 3-D.

ATOM-PROBE TOMOGRAPHIC STUDIES OF NICKEL-BASED ALLOYS

Nickel-based superalloys are used to fabricate single-crystal two-phase [γ'(L1$_2$) and γ(face-centered cubic)] turbine blades for aeronautical commercial and military jet engines, and land-based gas-turbine engines for generating electrical power; a single unit can generate as much as 500 MW. The single-crystal two-phase turbine blades are directionally solidified from different commercial or proprietary nickel-based superalloys and contain ten or more alloying elements. There is a continuing effort to increase the operating temperature of these turbine blades to increase the thermodynamic efficiency of the engines, which implies improving the high-temperature creep and oxidation resistance of these nickel-based superalloys. One route to improving the creep resistance is to decrease the coarsening rate of the coherent γ'(L1$_2$) precipitates, which
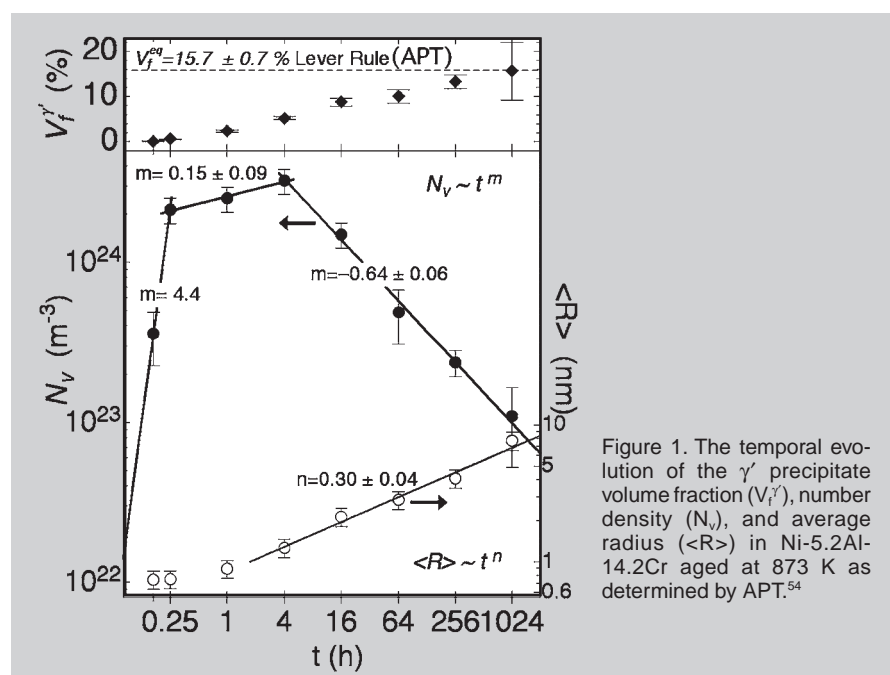

Figure 1. The temporal evolution of the γ' precipitate volume fraction ($V_f^{\gamma'}$), number density (N_v), and average radius ($<R>$) in Ni-5.2Al-14.2Cr aged at 873 K as determined by APT.[54]

The 3-D Computational Modeling of Shear-Dominated Ductile Failure in Steel*

Franck J. Vernerey, Canal McVeigh, Wing Kam Liu, Brian Moran, Deepti Tewari, David M. Parks, and Gregory. B. Olson

This paper presents recent advances in the computational analysis of the failure mechanisms in high-strength steel. Computational issues are described regarding modeling of the geometry, distribution, and material behavior of the dispersed phases present in the microstructure of steel. The investigation of the failure mechanisms using computational cell model methodology in two and three dimensions is then presented with an emphasis on microvoid-induced shear failure occurring at the scale of sub-micrometer grain-refining carbide precipitates. The failure of a three-dimensional particle cluster extracted from tomographic analysis of an engineering alloy is simulated. Finally the cell model results are used to simulate the failure of the material at the macro-scale.

INTRODUCTION

The ductility of high-strength steels is often restricted by the onset of a void-sheet mechanism in which failure occurs by a micro-void shear localization process. As part of a "Digital 3-D" consortium effort combining tomographic characterization with three-dimensional (3-D) simulation of realistic microstructures, a micro-void shear instability mechanism is identified here by examining the interactions occurring within a system of multiple embedded secondary particles (carbides, diameter ~10–100 nm) through a finite-element based computational cell modeling technique in two and three dimensions. Shear deformation leads to the nucleation of micro-voids as the secondary particles debond from the surrounding alloy matrix. The nucleated micro-voids grow into elongated void-tails along the principal shear plane and coalesce with the micro-voids nucleated at neighboring particles. The mechanism is incorporated

mathematically into a hierarchical model for deformation and failure of steel. The simulated response corresponds to experimentally observed behavior only when the micro-void shear localization mechanism is explicitly considered. The mechanism is explored in further detail through calculations carried out on a cluster of grain-refining carbide particles selected from a model tomographic data set obtained from an IN100 nickel alloy.[1,2]

See the sidebar for details on modeling of the microstructure.

INVESTIGATION OF FRACTURE MECHANISMS

Most of the knowledge regarding fracture mechanisms in steel is a result of observation of fracture surfaces. A typical fracture surface micrograph displays a dimpled structure that gives great insights on the distinct roles of primary and secondary particles. However, this technique gives only a qualitative explanation of the multiple phenomena arising in the failure process and sometimes fails to provide the nature of certain mechanisms, such as in a state of pure shear. This motivates the use of computational mechanics as a tool to investigate mechanisms and to better understand their relations to material microstructures. In this study, computational simulations based on unit-cell models are the primary means by which the micromechanics of the failure process have been investigated.

Figure 1. A hierarchical model for high-strength steels, showing three characteristic scales: the atomic scale to assess the debonding of particles, the scale of microvoid-nucleating secondary particles, and the scale of primary void-forming inclusion particles.

Multiple dispersed phases in a high-strength low-carbon steel: An atom-probe tomographic and synchrotron X-ray diffraction study

Michael D. Mulholland* and David N. Seidman

Northwestern University, Department of Materials Science and Engineering, Evanston, IL 60076 1928, USA

The co precipitation of Cu, M_2C (where M is any combination of Cr, Mo or Ti) and austenite (face centered cubic) is charac terized for 5 h isochronal aging times by synchrotron X ray diffraction and three dimensional atom probe tomography for a high strength low carbon steel, BlastAlloy 160. High number densities, $\sim 10^{23}$ m^{-3}, of co located Cu and M_2C precipitates were observed. Only small austenite volume percentages (<2.1%) were measured after aging at temperatures up to 625 °C for 5 h.
© 2009 Acta Materialia Inc. Published by Elsevier Ltd. All rights reserved.

Keywords: Three dimensional atom probe (3DAP); Steels; Copper precipitation

Strength and toughness generally have an inverse relationship in steels. It is therefore difficult to obtain steels that have both a high yield strength and a high impact toughness. Some demanding applications, such as pipelines and reactors, require just such a combination of properties. Naval applications also demand high-strength and excellent ductility and toughness for formability and explosion resistance. Additionally, naval steels must possess good weldability, which requires a high-strength low-carbon (HSLC) steel. HSLC steels have excellent weldability due to their low carbon content [1]. Such demanding mechanical properties are not met by normal steels. BlastAlloy (BA) 160 [2,3] is a HSLC steel that is designed to meet naval requirements. To achieve a 160 ksi (1103 MPa) yield strength, it employs Cu and M_2C (M is any combination of Cr, Mo, Ti and V) precipitation strengthening. Cu precipitation strengthening has been studied extensively in Fe Cu alloys [4 6] and in HSLA steels [7 10] but not in BA160. M_2C strengthening occurs in quenched and tempered martensitic steels and also creates a toughness increment due to cementite dissolution by M_2C precipitation [11]. M_2C precipitation has been characterized in ternary Fe Mo C and Fe W C alloys [12], in high-performance, high Ni Co alloy steels [13 17] and in high-speed steels [18] but not in BA160. Atom probe work on M_2C and other carbides is reviewed in Ref. [19].

To meet high toughness requirements, BA160 was designed to take advantage of transformation-induced plasticity (TRIP). TRIP is plastic deformation that is achieved by a phase transformation. Interaction of this transformation plasticity with fracture-controlling processes, such as shear localization, can delay shear instability and fracture to higher strains, resulting in enhanced toughness [20]. TRIP is usually accomplished through the transformation of austenite (face-centered cubic (fcc)) to martensite (body-centered tetragonal (bct)). Austenite or γ-Fe is the high temperature fcc Fe phase. The volume fraction and stability of γ-Fe are critical for determining the toughness increase due to TRIP [21]. Some γ-Fe is retained after thermomechanical processing, but more is needed for a toughness increment due to TRIP. Additional more stable dispersed γ-Fe can be precipitated in a controlled manner by reheating the steel into the $\gamma + \alpha$ (body-centered cubic (bcc)) two-phase field. Retained and precipitated γ-Fe morphologies have been studied in steels [22 24].

Although these different types of precipitates have received attention in other steels, the precipitation of all three phases in BA160 has been little studied [2,25]. The research presented herein characterizes precipitation of all three phases after isochronal aging using three-dimensional (3-D) local-electrode atom-probe (LEAP) tomography and synchrotron X-ray diffraction (XRD).

The composition of BA160 is given in Table 1. BA160 steel is formed into 8 in. (20.5 cm) ingots by vacuum induction melting and vacuum arc remelting. The ingots

---

Voltage-pulsed and laser-pulsed atom-probe-tomography of a multiphase high-strength low-carbon steel

Michael D. Mulholland[a] and David N. Seidman[a,b]

[a]Department of Materials Science and Engineering, Northwestern University, Evanston, IL 60208-3108, USA

[b]Northwestern University Center for Atom Probe Tomography (NUCAPT), Evanston, IL 60208-3108, USA

Abstract

The differences in artifacts associated with voltage-pulsed and laser-pulsed (wavelength = 532 or 355 nm) atom-probe tomographic (APT) analyses of nanoscale precipitation in a high-strength low-carbon steel are assessed using a local-electrode atom-probe (LEAP) tomograph. It is found that the interfacial width of nanoscale Cu precipitates increases with increasing specimen apex temperatures induced by higher laser pulse-energies (0.6-2 nJ pulse^{-1} at a wavelength of 532 nm). This effect is probably due to surface diffusion of Cu atoms. Increasing the specimen apex temperature by using pulse energies up to 2 nJ pulse^{-1} at a wavelength of 532 nm is also found to increase the severity of the local magnification effect for nanoscale M_2C metal carbide precipitates, which is indicated by a decrease of the local atomic density inside the carbides from 68 ± 6 nm^{-3} (voltage-pulsing) to as small as 3.5 ± 0.8 nm^{-3}. Methods are proposed to solve these problems based on comparisons with the results obtained from voltage-pulsed APT experiments. Essentially, application of the Cu precipitate compositions and local atomic-density of M_2C metal carbide precipitates measured by voltage-pulsed APT to 532 or 355 nm wavelength laser-pulsed data permits correct quantification of precipitation.

Introduction

The addition of laser pulsing to atom-probe tomography (APT) expands the range of materials that can be analyzed by APT (Gorelikov, 2000; Kellogg, 1987; Kellogg & Tsong, 1980; Tsong, 1978). Research projects that would be impossible to conduct using voltage-pulsed APT are now becoming numerous (Cerezo et al., 2007a; Chen et al., 2009; Chiaramonti et al., 2008; Gault et al., 2007; Kelly et al., 2007; Kelly & Miller, 2007; Larson et al., 2004; Li et al., 2010; Moutanabbir et al., 2011; Mulholland & Seidman, 2009; Schreiber et al., 2010a; Schreiber

ELSEVIER

Nanoscale co-precipitation and mechanical properties of a high-strength low-carbon steel

Michael D. Mulholland [a], David N. Seidman [a,b,*]

[a] *Department of Materials Science and Engineering, Northwestern University, Evanston, IL 60208 3108, USA*
[b] *Northwestern University Center for Atom Probe Tomography (NUCAPT), Evanston, IL 60208 3108, USA*

Abstract

Nanoscale co precipitation in a novel high strength low carbon steel is studied in detail after isothermal aging. Atom probe tomog raphy is utilized to quantify the co precipitation of co located Cu precipitates and M_2C (M is any combination of Cr, Mo, Fe, or Ti) carbide strengthening precipitates. Coarsening of Cu precipitates is offset by the nucleation and growth of M_2C carbide precipitate, resulting in the maintenance of a yield strength of 1047 ± 7 MPa (152 ± 1 ksi) for as long as 320 h of aging time at 450 °C. Impact ener gies of 153 J (113 ± 6 ft lb) and 144 J (106 ± 2 ft lb) are measured at 30 °C and 60 °C, respectively. The co location of Cu and M_2C carbide precipitates results in non stationary state coarsening of the Cu precipitates. Synchrotron source X ray diffraction studies reveal that the measured 33% increase in impact toughness after aging for 80 h at 450 °C is due to dissolution of cementite, Fe_3C, which is the source of carbon for the nucleation and growth of M_2C carbide precipitates. Less than 1 vol.% austenite is observed for aging treatments at temperatures less than 600 °C, suggesting that transformation induced plasticity does not play a significant role in the toughness of specimens aged at temperatures less than 600 °C. Aging treatments at temperatures greater than 600 °C produce more austenite, in the range 2 7%, but at the expense of yield strength.

1. Introduction

High-strength low-carbon (HSLC) steels are technolog ically important due to their excellent weldability and formability at considerably higher strength levels than con ventional steels with the same carbon concentrations [1,2]. Because of their high-strength and toughness values, HSLC steels often find use in demanding applications, such as high-strength pipelines, reactor vessels, and naval vessels. Naval applications require high-strength, excellent ductil ity, and high-toughness at −60 °C, which are critical for blast resistance; they also require good weldability for join ing steel plates. One HSLC steel designed specifically to meet the US Navy's specifications is BlastAlloy (BA) 160 [3,4], which employs a combination of Cu and M_2C (M is any combination of Cr, Mo, Fe, or Ti) carbide precipi tates to achieve a yield strength of 1103 MPa (160 ksi), a Charpy impact energy as high as 186 J (137 ± 7 ft-lb) at room temperature and 144 J (106 ± 2 ft-lb) at −60 °C, and a room temperature reduction in area >60%, prior to fracturing. Copper precipitation strengthening has been studied extensively in Fe Cu binary and ternary alloys [5 12], high-strength low-alloy (HSLA) steels [13 18], and a modified gear steel [19], whereas Cu precipitation in BA-160 has been studied only to a limited extent [4].

M_2C carbide strengthening occurs in quenched and tem pered martensitic steels with appropriate Mo and/or W concentrations and increases in toughness due to the disso lution of cementite (Fe_3C) and the concomitant precipita tion of M_2C carbide precipitates [20]. M_2C carbide

* Corresponding author at: Department of Materials Science and Engineering, Northwestern University, Evanston, IL 60208 3108, USA.
E mail address: d seidman@northwestern.edu (D.N. Seidman).

Multi-scale micromorphic theory for hierarchical materials

Franck Vernerey[a],*, Wing Kam Liu[b],**, Brian Moran[a]

[a]Department of Civil and Environmental Engineering, Northwestern University, 2145 Sheridan Road, Evanston, IL 60208-3111, USA
[b]Department of Mechanical Engineering, Northwestern University, 2145 Sheridan Road, Evanston, IL 60208-3111, USA

Abstract

For the design of materials, it is important to faithfully model macroscopic materials response together with mechanisms and interactions occurring at the microstructural scales. While brute force modeling of all the details of the microstructure is too costly, many of the current homogenized continuum models suffer from their inability to capture the correct underlying deformation mechanisms—especially when localization and failure are concerned. To overcome this limitation, a multi-scale continuum theory is proposed so that kinematic variables representing the deformation at various scales are incorporated. The method of virtual power is then used to derive a system of coupled governing equations, each representing a particular scale and its interactions with the macro scale. A constitutive relation is then introduced to preserve the underlying physics associated with each scale. The inelastic behavior is represented by multiple yield functions, each representing a particular scale of microstructure, but collectively coupled through the same set of internal variables. The theory is illustrated by two applications. First, a one-dimensional example of a three-scale material is presented. After the onset of softening, the model shows that the localization zone is distributed according to two distinct length scale determined by the model. Second, a two-scale continuum model is introduced for the failure of porous metals. By comparing the theory to a direct

---

*Corresponding author.
**Also to be corresponded to.
E-mail addresses: f-vernerey@northwestern.edu (F. Vernerey), w-liu@northwestern.edu (W.K. Liu).

ELSEVIER

Linking microstructure and properties through a predictive multiresolution continuum

Cahal McVeigh, Wing Kam Liu*

Department of Mechanical Engineering, Northwestern University, 2145 Sheridan Road, Evanston, IL 60208, United States

Abstract

Under the sponsorship of the NSF/Sandia Life Cycle Science based Engineering Program, the Sandia Predictive Science Program, and the ONR Digital 3D (D3D) program, a multiresolution continuum theory [C. McVeigh, F. Vernerey, W.K. Liu, L.C. Brinson, Comput. Methods Appl. Mech. Engrg. 195 (2006) 5053] is developed to predict material response when spatial and temporal microstructure evolution gives rise to severely inhomogeneous deformation at multiple scales. The proposed theory is applied by concurrently homogenizing the microstructure at each characteristic length scale associated with the inhomogeneous response. A continuum microstructure work rate equivalence approach is used to develop a set of continuum partial differential governing equations, in terms of multiresolution microstresses (and couple microstresses). Constitutive models relating to each microstress are determined from numerical microstructure models.

The multiresolution governing equations can be solved with a conventional finite element approach. Hence numerical and modeling errors analyses, probabilistic and reliability analyses and petaflop computing can be considered using existing approaches (or with transparent modifications). When only a single scale of inhomogeneous deformation (at the scale of the RVE) is considered, the multiresolution theory decomposes to the strain gradient theory of Fleck and Hutchinson. The theory is applied to (i) an alloy with two scales of statistically embedded particles, (ii) a cemented carbide and (iii) adiabatic shear banding in steel alloys. Only the mean constitutive behavior is considered at each scale; the full probabilistic analysis will be presented in a separate paper.
© 2008 Elsevier B.V. All rights reserved.

Keywords: Multiscale; Microstructure; Failure; Continuum; Gradient

1. Introduction

Predicting microstructure property relationships in engineering materials via direct simulation of the underlying micromechanics remains an elusive goal due to the massive disparities in length and time scales; huge structures such as bridges may fail after decades of operation due to nanoscale fracture events which occur at a micro/nano second time scale. Even as we move into the era of petaflop computing, affordability remains a key factor when developing a numerical analysis method.

In an effort to bypass the limitations of computational speed and storage capacity, engineers in many fields have focused on *multiscale* analysis theories. In the current paper we are interested in a multiscale theory which predicts macroscale mechanical deformation in terms of the underlying evolving microstructure. This type of approach usually involves coupling between simulations at different scales. If information is passed from one simulation (scale) to another in one direction only, it is known as a *hierarchical* approach. If information is exchanged in both directions between simulations (scales), the simulations must be performed *concurrently*. The hierarchical and concurrent approaches are explained further here. The multiresolution continuum theory proposed in this paper shares characteristics of both approaches.

* Corresponding author. Tel.: +1 847 491 7094.
  E mail address: w liu@northwestern.edu (W.K. Liu).

A multiresolution continuum simulation of the ductile fracture process

Rong Tian [a,1], Stephanie Chan [b], Shan Tang [a], Adrian M. Kopacz [a], Jian-Sheng Wang [c], Herng-Jeng Jou [c], Larbi Siad [d], Lars-Erik Lindgren [e], Gregory B. Olson [b], Wing Kam Liu [a,*]

[a] Department of Mechanical Engineering, Northwestern University, 2145 Sheridan Rd., Evanston, IL 60208, USA
[b] Department of Materials Science and Engineering, Northwestern University, 2220 Campus Dr., Evanston, IL 60208, USA
[c] QuesTek Innovations LLC, 1820 Ridge Ave., Evanston, IL 60201, USA
[d] Université de Reims, UFR Sciences Exactes et Naturelles, 51687 Reims Cedex 2, France
[e] Division of Material Mechanics, Lulea University of Technology, 971 87 Lulea, Sweden

ABSTRACT

With the advancement in computational science that is stepping into the Exascale era and experimental techniques that enable rapid reconstruction of the 3D microstructure, quantitative microstructure simulations at an unprecedented fidelity level are giving rise to new possibilities for linking microstructure to property. This paper presents recent advances in 3D computational modeling of ductile fracture in high toughness steels. Ductile fracture involves several concurrent and mutually interactive mechanisms at multiple length scales of microstructure. With serial sectioning tomographic techniques, a digital dataset of microstructure features associated with the fracture process has been experimentally reconstructed. In this study, primary particles are accurately and explicitly modeled while the secondary particles are modeled by a two scale multiresolution continuum model. The present numerical simulation captures detailed characteristics of the fracture process, such as zigzag crack morphology, critical void growth ratios, local stress triaxiality variation, and intervoid ligament structure. For the first time, fracture toughness is linked to multiscale microstructures in a realistic large 3D model.

1. Introduction

A severe limitation of existing modeling and CAE systems is the inability to seamlessly address the multiscale nature of the material/structural responses required to predict structural response in transient extreme environments. As depicted in Fig. 1, the damage evolution at a critical location (hot spot) of an aerospace structural system, which is made of two phase (for strength and toughness) alloys or composites, is a combination of microstructural events at multiple length scales. In this illustration, the macroscopic stress initiates the nucleation and growth of voids, creating an intense strain field between voids. Within the microstrain field, microvoids nucleate on finer secondary particles and microvoid growth

---

Prediction of Ductile Fracture Toughness

J.-S. Wang[1] and G. B. Olson[1, 2]
[1]_QuesTek Innovations LLC, Evanston, USA;_ [2]_Northwestern University, Evanston, USA_

Abstract
Inspired by recent multiscale modeling of void/microvoid interaction in ductile fracture, a new analysis of literature data on ultrahigh strength martensitic steels shows that J_{IC} toughness normalized by primary inclusion mean spacing is parabolically related to the measured critical primary void size ratio. Interpreting this critical ratio as a measure of the critical intervoid ligament strain for primary void coalescence by finer scale microvoid instability, calculation of the critical strain from Rice-Tracey void growth shows that J_{IC} toughness is exponentially related to the critical microvoid instability strain. This represents a far stronger sensitivity to critical strain than the previously assumed linear scaling. An approximate correlation of this critical strain to macroscopic fracture ductility allows an estimate of fracture toughness.

1. Introduction

Prediction of ductile fracture toughness, numerically or analytically, from microstructural and constitutive parameters has been a long-standing goal of the materials science and solid mechanics communities. Metallographic studies and recent multiscale simulations [1-6] show that 3D ductile fracture starts with plastic deformation followed by nucleation and growth of primary voids, and completes through primary void coalescence by a mechanism of intervoid ligament mechanical instability driven by interactive microvoiding on submicron-scale particles. New mechanistic insights provide an opportunity for reinterpretation of available literature data.

The mode I J-integral ductile fracture toughness is proportional to the critical crack tip opening displacement, δ_{IC}, and the flow stress σ_0 (usually taken to be the average of the yield strength and UTS) [7]:

$$J_{IC} = \frac{1}{d_n}\delta_{1C}\sigma_0$$

where $d_n\sim0.6$ depending on material deformation properties. Rice and Johnson [8] were the first to relate the crack tip opening displacement, δ_t, to inclusion microstructure. Based on a rigorous mechanics analysis at the crack tip, they derived that the true strain ahead of a crack tip is a function of a parameter X/δ_t, where X is the distance of a material point from the tip before deformation. Adopting a simple idea that some critical matrix fracture strain must be achieved at a material point initially at a distance X_0 from the crack tip, they concluded from numerical calculations that

DARPA / ONR D3D Final Summary Report (N00014-05-C-0241)
QuesTek Innovations LLC, 23 March 2011
PUBLICATION EXAMPLES - NOT FOR DISTRIBUTION
Page 44

1

M$_2$C Precipitation Strengthening in Steels

Jian-Sheng Wang[1] and Gregory B. Olson[1,2]

Abstract

Elastic interaction between nanoscaled coherent *M$_2$C* particles and dislocations in steels is analyzed based on equivalent eigenstrain method and analytical models of single-misfit-parameter. Both analyses show that coherent misfit dominates the interaction. To evade the burdensomeness of the eigenstrain method, a parameter called the constrained effective coherent misfit strain is introduced. With this parameter, Friedel-type shear-cutting model combining with Orowan bypassing appears to be sufficient to model the *M$_2$C* strengthening in steels. A modified analytical model of *M$_2$C* strengthening in steels is thus developed. Experimental data of *M$_2$C* precipitation strengthening in 510°C tempered 1605-type ultrahigh strength steels are reanalyzed with the modified model and compared with computer simulations and experimental data. It is concluded that 1) with the constrained effective coherent misfit strain, the modified analytic model are valid in analyzing *M$_2$C* strengthening in steels; 2) Orowan mechanism dominates *M$_2$C* particle strengthening, shear cutting occurs only if the particle is sub-nanometer in diameter and a peak stress as high as 1.2 GPa can be reached.

Introduction

Nanometer scaled *M$_2$C* carbide is the most important strengthening phase in ultrahigh strength steels, where *M* stands for transition metals, Cr, Mo and Fe. The strengthening mechanism of *M$_2$C* particles has been studied extensively[3, 4]. Hardness peaks were observed at particle sizes around 3 nm in diameter in 510 ºC tempered 1605 type steels, as shown in Figure 1. The steels were designed so that the driving force for *M$_2$C* precipitation increases from 1605-2B, 1605-2C to 1605-2D. Compositions of the steels are given in Table 1. Wise [3] concluded that the hardness peaks corresponded to a transition of the strengthening mechanism from shear cutting to Orowan bypassing and the modulus misfit between *M$_2$C* and the matrix dominated the shear cutting with the mechanism suggested by Hornbogen and Gahr[5].

Table 1 Compositions of experimental ultrahigh strength steels

Alloy	Co	Ni	Cr	Mo	C	Fe
1605-2D	15.99	4.96	0.02	4.03	0.24	bal.
1605-2C	16.08	4.97	0.71	2.82	0.24	bal.
1605-2B	16.09	4.98	1.4	1.52	0.24	bal.

[1] QuesTek Innovations LLC, Evanston, IL 60201

[2] Northwestern University, Evanston, IL 60201

[3] J.P. Wise, *Systems Design of Advanced Gear Steels*, Ph. D. thesis, Northwestern University, 1998.

[4] P. Jemian and J. R. Weertman, Unpublished research, Northwestern University, 1992.

[5] E. Hornbogen and K. A. Gahr, Metallography, 8, 181-202, 1975.

MECHANISM OF BCC-CU PARTICLE STRENGTHENING IN STEELS

Jian-Sheng Wang[1], and Gregory B. Olson[1,2]

Abstract: A new model for bcc-Cu particle strengthening in steels is proposed in view of the twined martensitic transformation with the increase in the precipitate size. This model is based on the concept that the particle/dislocation interaction promotes the phase transformation and the stress required for the transformation competing with the dislocation pileup stress at the particle/matrix interface. Predictions of the model are consistent with experimental data.

Introduction

Precipitation of bcc-Cu particles provides an additional strengthening in steels. The strengthening effect is less than that of M_2C particles as demonstrated in Figure 1. It is noticed that Orowan mechanism does not apply for bcc-Cu particles, as reported in [1] that Cu-particle strengthening over a wide aging range is less than the Orowan stress indicating dislocations shear cutting large bcc-Cu particles before Orowan looping.
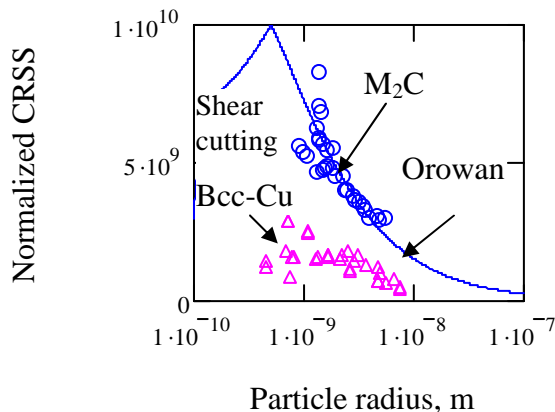

Figure 1 M_2C and bcc-Cu strengthening in steels. The blue line and circles are the model prediction and experimental data for M_2C particles [2], respectively; purple triangles are experimental data for bcc-Cu particles [1,3,4,]. CRSS denotes the increase in the critical resolved shear stress. CRSS are normalized by a parameter related the square root of the particle volume fraction so that data with various volume factions are comparable.

Since the publication of the Russell-Brown model in the early 1970's [5] it had been widely believed that bcc-Cu particle strengthening in steels was originated from the modulus misfit between copper and iron. The validity of the Russell-Brown model was challenged recently, although based on false basis. For example, Fine and Isheim [6] pointed out that the R-B model would predict very weak strengthening, but the equations they cited are incorrect. Based on molecular dynamics simulations, Harry and Bacon concluded that "metastable bcc-Cu is elastically harder than α-iron, rather than softer" and proposed a dislocation core interaction model [7]. First-principles calculations, however, showed that the tetragonal shear modulus $C'=(C_{11}-C_{12})/2$ for metastable bcc-Cu is negative [8,9]; metastable bcc-Cu is softer than α-Fe.

With the value of shear modulus μ = 22.3 GPa and lattice parameter a = 0.289 nm (Appendix-1), predictions of the R-B model, together with Friedel shear-cutting (Appendix-2) and Orowan bypassing stresses (Appendix-3) in comparison with experimental data are shown in Figure 2. None of the models consists with experimental

---

Nanoscale co-precipitation and mechanical properties of a high-strength low-carbon steel

Michael D. Mulholland[a] and David N. Seidman[a,b,*]

[a]Department of Materials Science and Engineering, Northwestern University, Evanston, IL 60208-3108, USA
[b]Northwestern University Center for Atom Probe Tomography (NUCAPT), Evanston, IL 60208-3108, USA

Abstract

Nanoscale co-precipitation in a novel high-strength low-carbon steel is studied in detail after isothermal aging. Atom-probe tomography is utilized to quantify the co-precipitation of co-located Cu precipitates and M_2C (M is any combination of Cr, Mo, Fe, or Ti) carbide strengthening precipitates. Coarsening of Cu precipitates is offset by the nucleation and growth of M_2C carbide precipitate, resulting in the maintenance of a yield strength of 1047 ± 7 MPa (152 ± 1 ksi) for as long as 320 h of aging time at 450 °C. Impact energies of 153 J (113 ± 6 ft-lbs) and 144 J (106 ± 2 ft-lbs) are measured at -30 °C and – 60 °C, respectively. The co-location of Cu and M_2C precipitates results in non-stationary state coarsening of the Cu precipitates. Synchrotron-source x-ray diffraction studies reveal that the measured 33% increase in impact toughness after aging for 80 h at 450 °C is due to dissolution of cementite, Fe_3C, which is the source of carbon for the nucleation and growth of M_2C carbide precipitates. Less than 1 volume percent austenite is observed for aging treatments at temperatures less than 600 °C, suggesting that TRIP does not play a significant role in the toughness of specimens aged at temperatures less than 600 °C. Aging treatments at temperatures greater than 600 °C produce more austenite, in the range 2-7%, but at the expense of yield strength.

Key Words:

*Corresponding author: d-seidman@northwestern.edu

THE 3D EFFECTS IN NANO-PARTICLE STRENGTHENING

J.-S. Wang[1], H.-J. Jou[1] and G. B. Olson[1,2]

[1]QuesTek Innovations LLC, [2]Northwestern University

The 3D analytic models for nano-particle strengthening

3D particle size distribution parameters

The effect of the 3D particle size distribution is induced in the analytical model by introducing Numbach's size distribution parameters, which are defined with 1 to 6 orders of momentum of the distribution density function[1]. The distribution density for Wagner-Lifshitz-Slyozov (WLS) distribution and log-normal distribution with various variances is shown in Figure 1. From the analytical model and verified by computer simulations, the wide spread size distribution reduces the Orowan stress, while the shear cutting stress is increased slightly. LEAP measurements show that both bcc-Cu and M_2C particles follow log-normal distribution, but bcc-Cu particles with less variance (~0.25) than that of M_2C particles and variation increases with aging time. Therefore, the strengthening capability of M_2C particles decreases with aging time, while the capability of bcc-Cu strengthening does not change with aging time.
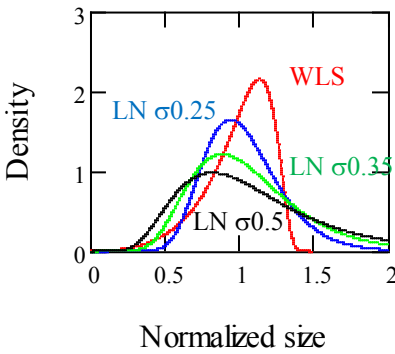
Figure 1 Distribution density

Effect of size distribution in analytical models is characterized by parameters ω_r, ω_q and ω_d, which are defined by the 1 to 3 order of momentum of the size distribution function. The mean size of particles at the slip plane is given by

$$r_r = r\omega_r$$

The edge-to-edge near-neighbor spacing is

$$\lambda = \left(\sqrt{\frac{\pi\omega_q}{f}} - 2\omega_r \right) r$$

The area number density at the slip plane is

---

[1] E. Nembach, Particle Strengthening of Metals and Alloys, John Willey & Sons, Inc., New York, 1997

Rajesh Prasannavenkatesan
George W. Woodruff School of Mechanical Engineering,
Georgia Institute of Technology,
Atlanta, GA 30332-0405

David L. McDowell[1]
George W. Woodruff School of Mechanical Engineering, and School of Materials Science and Engineering,
Georgia Institute of Technology,
Atlanta, GA 30332-0405
e-mail: david.mcdowell@me.gatech.edu

Gregory B. Olson
Department of Materials Science and Engineering,
Robert R. McCormick School of Engineering and Applied Science,
Northwestern University,
Evanston, IL 60208-3108;
Questek Innovations LLC,
Evanston, IL 60201

Herng-Jeng Jou
Questek Innovations LLC,
Evanston, IL 60201

Modeling Effects of Compliant Coatings on HCF Resistance of Primary Inclusions in High Strength Steels

Nucleation of fatigue cracks at nonmetallic primary inclusions in high cycle fatigue of martensitic steel is computationally investigated. We explore the capabilities of an elastic interphase material adhered to the inclusion surface to alter the driving force for fatigue crack nucleation in the matrix. By varying the elastic stiffness of the encapsulating interphase, the stresses and cyclic plastic strains are examined in the matrix in the proximity of a partially debonded inclusion, a worst case scenario for nucleation. The matrix is modeled as elastic-plastic with pure kinematic hardening expressed in a hardening minus dynamic recovery format. The inclusion and interphase are modeled as isotropic linear elastic. An idealized spherical, homogeneous inclusion is considered to facilitate parametric study. A nonlocal average value of the maximum plastic shear strain amplitude was used in a modified form of the Fatemi–Socie parameter in the proximity of inclusions as a fatigue indicator parameter to facilitate comparative parametric study of potency for crack nucleation. [DOI: 10.1115/1.3030943]

Keywords: inclusion, fatigue crack, interphase, high cycle fatigue

1 Introduction

Design of improved process routes and new material systems that address the increasing demand for extended fatigue performance in technologically significant structural materials is a key research focus. Nonmetallic primary inclusions are a major life-limiting feature in advanced metallic systems. Simulation-based strategies offer a convenient platform to understand mechanisms of crack nucleation and growth from such second phase particles [1,2], which in turn can be applied to develop understanding of possible means to suppress such phenomena.

The mechanisms of crack nucleation and early growth from inclusion involve either cracking of the inclusion or debonding of the inclusion/matrix interface, with the inclusion serving as a notch to concentrate cyclic plastic strain in the surrounding metal matrix [3,4]. Of the three scenarios, decohesion of inclusion/matrix interface, either during processing or service, has been observed to be most detrimental with regard to fatigue crack nucleation in metals [3,5,6]. Gall et al. [5] reported for A356-T6 Al alloy that the fatigue crack driving force levels near perfectly bonded inclusions are two orders of magnitude smaller than that near cracked or debonded particles, within the range of elastic stiffness contrast and yield strengths studied. Due to high stress concentration, it is improbable that a cracked inclusion would remain completely bonded to the matrix material, and the cracked inclusion might eventually debond during service. Improving the inclusion/matrix interface strength is one way to negate or delay the process of decohesion. Another remedy would be to introduce an interphase layer between inclusion and matrix either to inhibit decohesion or to reduce stresses and plastic strain localization in

the matrix in the event of decohesion. In this paper we propose to study the effect of the latter by introducing an elastic interphase material that adheres to the inclusion surface, forming a layer between the inclusion and matrix.

The influence of such coatings on the structural response of different material systems has been studied by many researchers [7–14]. Interaction of pre-existing cracks and dislocations with coated particles (inclusions or fibers) has also been studied by many researchers [11,15–20]. Such second phase particles have often been reported to serve as crack nuclei in different grades of steel [3,21–25]. Gubenko [26] performed experiments to understand the interface characteristics between an inclusion and steel matrix. Based on the experimental findings on void formation from corundum and spinel inclusions, the author suggested to create silicate and sulfide shells around such second phase particles in order to lower the susceptibility of decohesion of the inclusion/matrix interface. Miao and Knott [27] performed experiments on C–Mn steel weld metal and demonstrated that by heating the steel to austenitization temperature followed by slow cooling resulted in formation of sulfide coating (MnS) on oxide inclusions with thickness ranging between 0.1 μm and 0.5 μm. Manganese sulfide is relatively less stiff than oxide inclusion and hence can be viewed as a compliant coating layer between the steel matrix and the oxide particle. In comparison to the bulk materials, thin coatings exhibit strong anisotropy in mechanical properties [28,29]. Additionally, the properties of substrate can influence the mechanical behavior of coatings [30]. Although the aforementioned factors can influence the severity of plastic strain localization in the surrounding ductile matrix, detailed investigation of their effects is beyond the scope of this paper.

The effect of introducing such coatings on fatigue crack nucleation at nonmetallic inclusions in metals has not been explored to date. We examine the possible reduction in the driving force for fatigue crack nucleation in such a case for a parametric range of relative elastic stiffnesses of the inclusion, interphase, and matrix

---
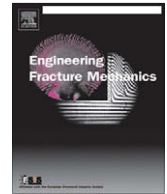
Modeling fatigue crack nucleation at primary inclusions in carburized and shot-peened martensitic steel

Jixi Zhang, Rajesh Prasannavenkatesan, Mahesh M. Shenoy, David L. McDowell *

The George W. Woodruff School of Mechanical Engineering, Georgia Institute of Technology, Atlanta, GA 30332-0405, USA

ABSTRACT

The mechanics of high cycle fatigue crack nucleation (formation of a stable crack that can grow away from the influence of the notch root of the inclusion) at subsurface primary inclusions in carburized and shot peened martensitic steel subjected to cyclic bending is investigated using three dimensional (3D) finite element (FE) analysis. FE models are con structed using a voxellation technique to address the shape, size, and distribution of pri mary inclusions within clusters. The critical depth for fatigue crack nucleation is predicted considering the gradient in material properties arising from carburization, pre strain and compressive residual stress distribution due to shot peening, and the gradient of applied bending stress. The influence of inclusion shape and interface condition (intact or debonded) with the matrix on the driving force for fatigue crack nucleation is examined. It is observed that the inclusion shape has minimal influence on the predicted results while the effect of the interface condition is quite significant. For partially debonded interfaces, the predicted critical depth from surface for fatigue crack nucleation agrees qualitatively with experimental observations.

© 2008 Elsevier Ltd. All rights reserved.

1. Introduction

Durability of gears and gear steels is critical to life expectancy of power transmission systems. One of the most common failure modes in gears is tooth bending fatigue, which accounts for 32% of all gear failures [1,2]. Improved understanding of fatigue behavior of gear steels is needed to properly design and use gears. Moreover, simulation based approaches can assist in design of process route to promote fatigue resistance.

Carburized steel gears shot peened to impart compressive surface residual stress are widely employed in industry [3]. By employing carburization followed by quenching process and low temperature tempering, it is possible to produce a hard case with a more ductile core to improve wear and fatigue resistance. Donzella et al. [4] found that fatigue strength increases with the increase of case depth. As a result of shot peening, fatigue cracks tend to form in the subsurface of carburized gears [3]. The effect of shot peening parameters on fatigue life of carburized gears has been systematically investigated [5 7].

Numerous factors affect the fatigue resistance of carburized steel. They include hardness, residual stress, surface finish, microstructure, grain size, globular and network carbides, intergranular oxidation, microcracking, and the presence of re tained austenite. Many of these factors interact to influence wear and fatigue performance [8]. Extensive experimental stud ies have shown that the three most effective ways to improve bending fatigue strength are (i) increasing the compressive residual stresses at the surface, (ii) refining the prior austenite grain size in the case region, and (iii) minimizing intergranular oxidation at prior austenite grain boundaries [9,10]. Among them, the effectiveness of shot peening ranks highest [11].

---

* Corresponding author. Tel.: +1 404 894 5128; fax: +1 404 894 0186.
  E-mail address: david.mcdowell@me.gatech.edu (D.L. McDowell).

3D modeling of subsurface fatigue crack nucleation potency of primary inclusions in heat treated and shot peened martensitic gear steels

Rajesh Prasannavenkatesan [a], Jixi Zhang [c], David L. McDowell [a,b,*], Gregory B. Olson [d,e], Herng-Jeng Jou [e]

[a] George W. Woodruff School of Mechanical Engineering, Georgia Institute of Technology, Atlanta, GA 30332-0405, USA
[b] School of Materials Science and Engineering, Georgia Institute of Technology, Atlanta, GA 30332-0245, USA
[c] Department of Mechanical Engineering, University of Nevada, Reno, NV 89557, USA
[d] Department of Materials Science and Engineering, Robert R. McCormick School of Engineering and Applied Science, Northwestern University, Evanston, IL 60208-3108, USA
[e] Questek Innovations LLC, Evanston, IL 60201, USA

ABSTRACT

A computational strategy is developed to characterize the driving force for fatigue crack nucleation at subsurface primary inclusions in carburized and shot peened C61® martensitic gear steels. Experimental investigation revealed minimum fatigue strength to be controlled by subsurface fatigue crack nucleation at inclusion clusters under cyclic bending. An algorithm is presented to simulate residual stress distribution induced through the shot peening process following carburization and tempering. A methodology is developed to analyze potency of fatigue crack nucleation at subsurface inclusions. Rate independent 3D finite element analyses are performed to evaluate plastic deformation during processing and service. The specimen is subjected to reversed bending stress cycles with $R \approx 0.05$, representative of loading on a gear tooth. The matrix is modeled as an elastic–plastic material with pure nonlinear kinematic hardening. The inclusions are modeled as isotropic, linear elastic. Idealized inclusion geometries (ellipsoidal) are considered to study the fatigue crack nucleation potency at various subsurface depths. Three distinct types of second phase particles (perfectly bonded, partially debonded, and cracked) are analyzed. Parametric studies quantify the effects of inclusion size, orientation and clustering on subsurface crack nucleation in the high cycle fatigue (HCF) or very high cycle fatigue (VHCF) regimes. The nonlocal average values of maximum plastic shear strain amplitude and Fatemi–Socie (FS) parameter calculated in the proximity of the inclusions are considered as the primary driving force parameters for fatigue crack nucleation and microstructurally small crack growth. The simulations indicate a strong propensity for crack nucleation at subsurface depths in agreement with experiments in which fatigue cracks nucleated at inclusion clusters, still in the compressive residual stress field. It is observed that the gradient from the surface of residual stress distribution, bending stress, and carburized material properties play a pivotal role in fatigue crack nucleation and small crack growth at subsurface primary inclusions. The fatigue potency of inclusion clusters is greatly increased by prior interfacial damage during processing.

© 2008 Elsevier Ltd. All rights reserved.

1. Introduction

Although much progress has been made, development of quantitative descriptions of potency of primary inclusions for fatigue crack nucleation and early stages of growth in high strength steels requires further understanding to support quantitative materials design. Carburization and shot peening are well established techniques for improving high cycle fatigue strength of steel components [1–7]. The fact that bending fatigue strength of steel gear teeth is increased considerably by carburization and shot peening has been extensively utilized in industry [8–11]. With carburization and shot peening, crack initiation (nucleation and early growth at the scale of the primary inclusion) is observed to shift from the surface toward the subsurface of the carburized gears; this is primarily due to presence of high compressive residual stress and comparatively high hardness at the surface. It is widely observed that cracks in unnotched specimens nucleate at non-metallic inclusions and other microstructure inhomogeneities. Such second phase particles often serve as fatigue crack starters in a variety of metallic materials [12–18]. Extensive experimental observations have been reported earlier on subsurface crack initiation [19–23].

Toyada et al. [21] performed a series of rotating bending fatigue tests on Cr–Mo steels and estimated the influence of the inclusions on the fatigue strength by employing the projected $\sqrt{area}$

3D modeling of subsurface fatigue crack nucleation potency of primary inclusions in heat treated and shot peened martensitic gear steels

Rajesh Prasannavenkatesan [a], Jixi Zhang [c], David L. McDowell [a,b,*], Gregory B. Olson [d,e], Herng-Jeng Jou [e]

[a] George W. Woodruff School of Mechanical Engineering, Georgia Institute of Technology, Atlanta, GA 30332-0405, USA
[b] School of Materials Science and Engineering, Georgia Institute of Technology, Atlanta, GA 30332-0245, USA
[c] Department of Mechanical Engineering, University of Nevada, Reno, NV 89557, USA
[d] Department of Materials Science and Engineering, Robert R. McCormick School of Engineering and Applied Science, Northwestern University, Evanston, IL 60208-3108, USA
[e] Questek Innovations LLC, Evanston, IL 60201, USA

ARTICLE INFO

ABSTRACT

A computational strategy is developed to characterize the driving force for fatigue crack nucleation at subsurface primary inclusions in carburized and shot peened C61® martensitic gear steels. Experimental investigation revealed minimum fatigue strength to be controlled by subsurface fatigue crack nucleation at inclusion clusters under cyclic bending. An algorithm is presented to simulate residual stress distribution induced through the shot peening process following carburization and tempering. A methodology is developed to analyze potency of fatigue crack nucleation at subsurface inclusions. Rate independent 3D finite element analyses are performed to evaluate plastic deformation during processing and service. The specimen is subjected to reversed bending stress cycles with $R \approx 0.05$, representative of loading on a gear tooth. The matrix is modeled as an elastic–plastic material with pure nonlinear kinematic hardening. The inclusions are modeled as isotropic, linear elastic. Idealized inclusion geometries (ellipsoidal) are considered to study the fatigue crack nucleation potency at various subsurface depths. Three distinct types of second phase particles (perfectly bonded, partially debonded, and cracked) are analyzed. Parametric studies quantify the effects of inclusion size, orientation and clustering on subsurface crack nucleation in the high cycle fatigue (HCF) or very high cycle fatigue (VHCF) regimes. The nonlocal average values of maximum plastic shear strain amplitude and Fatemi–Socie (FS) parameter calculated in the proximity of the inclusions are considered as the primary driving force parameters for fatigue crack nucleation and microstructurally small crack growth. The simulations indicate a strong propensity for crack nucleation at subsurface depths in agreement with experiments in which fatigue cracks nucleated at inclusion clusters, still in the compressive residual stress field. It is observed that the gradient from the surface of residual stress distribution, bending stress, and carburized material properties play a pivotal role in fatigue crack nucleation and small crack growth at subsurface primary inclusions. The fatigue potency of inclusion clusters is greatly increased by prior interfacial damage during processing.

© 2008 Elsevier Ltd. All rights reserved.

1. Introduction

Although much progress has been made, development of quantitative descriptions of potency of primary inclusions for fatigue crack nucleation and early stages of growth in high strength steels requires further understanding to support quantitative materials design. Carburization and shot peening are well established techniques for improving high cycle fatigue strength of steel components [1–7]. The fact that bending fatigue strength of steel gear teeth is increased considerably by carburization and shot peening

has been extensively utilized in industry [8–11]. With carburization and shot peening, crack initiation (nucleation and early growth at the scale of the primary inclusion) is observed to shift from the surface toward the subsurface of the carburized gears; this is primarily due to presence of high compressive residual stress and comparatively high hardness at the surface. It is widely observed that cracks in unnotched specimens nucleate at non-metallic inclusions and other microstructure inhomogeneities. Such second phase particles often serve as fatigue crack starters in a variety of metallic materials [12–18]. Extensive experimental observations have been reported earlier on subsurface crack initiation [19–23].

Toyada et al. [21] performed a series of rotating bending fatigue tests on Cr–Mo steels and estimated the influence of the inclusions on the fatigue strength by employing the projected $\sqrt{\text{area}}$

Polycrystal Plasticity Modeling of Cyclic Residual Stress Relaxation in Shot Peened Martensitic Gear Steel

Rajesh Prasannavenkatesan
QuesTek Innovations LLC,
Evanston, IL 60201;
George W. Woodruff School of Mechanical
Engineering,
Georgia Institute of Technology,
Atlanta, GA 30332-0405

David L. McDowell[1]
George W. Woodruff School of Mechanical
Engineering,
Georgia Institute of Technology,
Atlanta, GA 30332-0405;
School of Materials Science and Engineering,
Georgia Institute of Technology,
Atlanta, GA 30332-0405
e-mail: david.mcdowell@me.gatech.edu

Using a three-dimensional crystal plasticity model for cyclic deformation of lath martensitic steel, a simplified scheme is adopted to simulate the effects of shot peening on inducing initial compressive residual stresses. The model is utilized to investigate the subsequent cyclic relaxation of compressive residual stresses in shot peened lath martensitic gear steel in the high cycle fatigue (HCF) regime. A strategy is identified to model both shot peening and cyclic loading processes for polycrystalline ensembles. The relaxation of residual stress field during cyclic bending is analyzed for strain ratios $R_\varepsilon = 0$ and -1 for multiple realizations of polycrystalline microstructure. Cyclic microplasticity in favorably oriented martensite grains is the primary driver for the relaxation of residual stresses in HCF. For the case of $R_\varepsilon = -1$, the cyclic plasticity occurs throughout the microstructure (macroplasticity) during the first loading cycle, resulting in substantial relaxation of compressive residual stresses at the surface and certain subsurface depths. The initial magnitude of residual stress is observed to influence the degree (percentage) of relaxation. Describing the differential intergranular yielding is necessary to capture the experimentally observed residual stress relaxation trends. [DOI: 10.1115/1.4001594]

Keywords: lath martensite, residual stress, relaxation, crystal plasticity, shot peening

1 Introduction

It is well known that mechanical surface treatments, such as deep rolling, shot peening, and laser shock peening, can significantly improve the fatigue behavior of highly stressed metallic components [1,2]. This work focuses on compressive residual stress induced through shot peening. These stresses enhance the service life of the component by resisting fatigue crack formation and growth on and near the surface of the specimen. The residual stresses can relax significantly due to subsequent mechanical and/or thermal loading even under normal operating conditions. Measurements and effects of residual stresses have proven difficult to interpret in relation to influence on fatigue life. To a large extent, this uncertainty arises from the limitations associated with the surface measurements of residual stresses through the depth of the shot peened layer. There is also a lack of knowledge of the effect of fatigue cycling on such stresses since it is difficult to measure residual stress changes during cycling. Computational modeling such as finite element (FE) analysis offers a convenient platform to investigate the effects of process history (including residual stresses) on fatigue resistance of components. Considerable progress is being made in developing state-of-the-art techniques aimed at in situ characterization of the stress/strain evolution during cyclic loading [3,4]. Such experimental techniques will be helpful to calibrate and validate model predictions. There is considerable interest in developing improved fatigue life prediction models that incorporate residual stress effects [5–7].

Extensive experimental studies have been performed to understand the relaxation of compressive residual stresses induced through shot peening [8–11]. Accordingly, the relaxation during fatigue cycling can be divided into two stages: abrupt relaxation during the first cycle and gradual change in the following cycles [12]. It is conventionally held that residual stress relaxation due to mechanical loading occurs when the superposition of applied stress and residual stress exceeds the macroscopic yield strength of the material. Also, decrease in the yield strength with increase in temperature can promote residual stress relaxation. During service, cyclic hardening or softening due to repeated loading can alter the residual stress distribution [13]. The present work explores how short-range microplastic deformation during cyclic loading promotes relaxation of residual stresses at remote stress amplitudes well below the yield strength of the material, which is typical of high cycle fatigue (HCF) loading conditions. Almer et al. [14] pointed out that microstresses within grains relax rapidly during fatigue while macroscopic stress relaxes less rapidly; this significantly influences fatigue crack formation and growth behavior in HCF.

Modeling surface treatments such as shot peening is challenging and must be carried out using at least two levels. The process of shot peening involve bombarding the surface of the component with small spherical shots made of hardened cast-steel, conditioned cut-wire, glass, or ceramic beads at a relatively high impingement velocity (40–70 m/s). Surface impact processes are highly dynamic and stochastic. On the other hand, below the near surface layer, the process of constrained plastic deformation at each depth is amenable to rather simple approximation. The major focus has been on predicting the residual stress distribution from models to use in optimizing the shot peening process. Empirical methods based on experimental data have been suggested to model the residual stress distribution following shot peening [15,16]. The earliest work concerning modeling of shot peening was performed by Shaw and De Salvo [17], who performed quasistatic analyses of single shot and twin shots on plastic strain distribution. Similar approaches have been undertaken by many authors [18,19] to understand the effect of single shot on the stress and strain distribution on the specimen surface. The dynamic modeling of a single shot was initially conducted by Johnson [20]

PHYSICAL REVIEW LETTERS

Electronic Selection Rules Controlling Dislocation Glide in bcc Metals

Travis E. Jones,[1,*] Mark E. Eberhart,[2,+] Dennis P. Clougherty,[1,2] and Chris Woodward[3]

[1]*Molecular Theory Group, Colorado School of Mines, Golden, Colorado 80401, USA*
[2]*Department of Physics, University of Vermont, Burlington, Vermont 05405 0125, USA*
[3]*Materials and Manufacturing Directorate, Air Force Research Laboratories, Wright Patterson Air Force Base, Dayton, Ohio 45433 7817, USA*

The validity of the structure property relationships governing the low temperature deformation behav ior of many bcc metals was brought into question with recent *ab initio* density functional studies of isolated screw dislocations in Mo and Ta. These relationships were semiclassical in nature, having grown from atomistic investigations of the deformation properties of the group V and VI transition metals. We find that the correct form for these structure property relationships is fully quantum mechanical, involving the coupling of electronic states with the strain field at the core of long $a/2\langle 111\rangle$ screw dislocations.

Single crystal bcc metals show remarkable variation in their plastic anisotropy and glide properties. For example, the anisotropy ratio of Ta is twice that of Mo, and under antitwinning stress, Ta is characterized by anomalous glide along {112} planes. This variability must be rooted in the dislocations that mediate plastic behavior. In the case of bcc metals, where the edge and mixed character disloca tions are mobile even in the elastic regime, it is the long screw character $a/2\langle 111\rangle$ dislocations that are activated during plastic deformation. Hence, it is differences in the structure of these dislocations that was suspected to be responsible for the variations in plastic anisotropy and glide response of the bcc metals [1,2].

Atomistic calculations designed to elucidate the core structure of $a/2\langle 111\rangle$ dislocations [1,3–5] showed differ ences between the core structures of Mo and Ta. While the dislocation core of both metals was spread on three con jugate (110) planes, in Ta the spreading was symmetrical about the dislocation line, and for Mo it was asymmetric. Thus, the dislocation core of Ta was characterized by full $D3$ symmetry and Mo by an approximate threefold rotation axis, ($C3$).

Beigi and Arias [6] were the first to question this as sumption. Using electronic structure density functional theory (DFT) calculations to study closely spaced disloca tion dipole arrays, they found qualitative evidence of sym metric strain fields around $a/2\langle 111\rangle$ screw dislocations in Mo. More realistic and quantitative DFT studies [2,7,8] employing a flexible boundary condition also showed both Mo and Ta to be characterized by symmetric dislocation cores. Further, the calculated anisotropy ratio agreed with the limited experimental measurements, with a twinning antitwinning asymmetry ratio of 2 in Mo and 4 in Ta.

Despite the computational successes, the underlying structure(s) mediating the deformation properties of bcc metals remain elusive. Here, we show that the variations in glide properties at temperatures where thermally activated

dislocation motion is negligible are due to differences in the symmetry imposed coupling between electronic states and applied strain. The selection rules governing this cou pling are mediated by the topology of the total charge density at the cores of $a/2\langle 111\rangle$ screw dislocations. It is because Mo has one more valence electron than does Ta, that their charge density topologies, and consequent prop erties, are also different. (Though the variations in plastic anisotropy are also rooted in differences in electron count and charge density topology, this topic will be saved for a subsequent paper.)

The relationship between charge density topology and mechanical properties can be understood from the Hohenberg-Kohn theorem, which asserts that a system's ground-state properties are a consequence of its charge density, a scalar field denoted as $\rho(\vec{r})$ [9]. Bader [10] noted that the essence of a molecule's structure must be con tained within the topology of $\rho(\vec{r})$. The topology of a scalar field is given in terms of its critical points (CPs), which are the zeros of the gradient of this field. There are four kinds of CP in a three-dimensional space: a local minimum, a local maximum and two kinds of saddle point. These CPs are denoted by an index, which is the number of positive curvatures minus the number of negative curvatures. For example, a minimum CP has positive curvature in three orthogonal directions; therefore it is called a (3, 3) CP. The first number is simply the number of dimensions of the space, and the second number is the net number of positive curvatures. A maximum is denoted by (3, −3), since all three curvatures are negative. A saddle point with two of the three curvatures negative is denoted (3, −1), while the other saddle point is a (3, 1) CP. For the purposes of this paper, only the (3, −3) and (3, −1) CPs need further consideration.

Through extensive studies of molecules and crystals, Bader and Zou [11] and Bader [10] showed that it was possible to correlate topological properties of the charge

085505-1

The topologies of the charge densities in Zr and Ru

Travis E. Jones* and Mark E. Eberhart

Molecular Theory Group, Colorado School of Mines, Golden, Colorado 80401, USA. Correspondence e mail: trjones@mines.edu

We report on the atomic scale phenomena responsible for the variation of oxygen solubility in Zr and Ru. First-principles calculations reveal that the topologies of the charge densities in these hexagonal close-packed metals are distinct. Neither element was found to possess the topology of the prototype, Mg. There are 12 bond paths terminating at each Ru atom. These are the bonds between nearest neighbors. Only five bond paths terminate at each Zr atom and the Zr atoms are not bound to one another. Instead, they are bonded through non-nuclear maxima. As a result, channels of low charge density that can accommodate oxygen anions are present in Zr.

1. Introduction

Oxygen dissolves interstitially to the octahedral holes of hexagonal close-packed (h.c.p.) metals. However, the extent to which it dissolves, its solubility, is remarkably variable. The Group IV metals (Ti, Zr, Hf) are characterized by appreciable oxygen solubility of the order of 20 at.%. In contrast, oxygen is nearly insoluble in the Group VIII h.c.p. metals (Ru, Os). The underlying structure responsible for this remarkable variation arises from the different charge-density topologies of these metals.

The topological theory of molecular structure, the 'atoms in molecules' (AIM) theory, was first articulated by Bader. This theory has been applied to a variety of crystalline systems (Bader, 1990; Zou & Bader, 1994). The first application of AIM theory to the solid state revealed that there are no second-neighbor bonds in face-centered cubic (f.c.c.) transition metals (Eberhart *et al.*, 1991). Subsequent studies have supported that observation (Eberhart *et al.*, 1992; Kioussis *et al.*, 2002), and have also been extended to show that nonmagnetic body-centered cubic (b.c.c.) transition metals possess only first-neighbor bonds (Eberhart, 1996*a*). However, there is no reason why second-neighbor bonds should not exist. As Zou pointed out, the only symmetry requirement is that the non-nuclear critical points lie on the Wigner Seitz cell (Zou & Bader, 1994). Moreover, a more recent study of f.c.c. and b.c.c. iron has shown that second-neighbor bonds are present in magnetic transition metals (Jones, Eberhart & Clougherty, 2008).

This ability to unambiguously define bonds has made AIM theory a useful tool for the investigation of 'bonding' in materials ranging from high-temperature alloys to biological systems. These investigations have yielded interesting results. The geometry of the charge density at bond points was found to correlate with the single-crystal elastic moduli in f.c.c. and b.c.c. transition metals (Eberhart, 1996*a,b*). Second-neighbor bond paths were found in B2 ionic crystals (Luaña *et al.*, 1997)

and transition-metal aluminides (Eberhart & Giamei, 1998), with the magnitude of the latter correlating to failure properties (Eberhart, 2001). Second-neighbor bond paths were also found in iron, where a well known magnetic phase change was shown to be a topological phase transition (Jones, Eberhart & Clougherty, 2008). Other studies have used the geometry of the charge density at bond points to offer first-principles explanations of the anomalous behavior of iridium under shear (Kioussis *et al.*, 2002), as well as the motion of Ta and Mo screw dislocation cores (Jones, Eberhart, Clougherty & Woodward, 2008).

One of the attractive features of AIM theory is its reliance on the charge density, a quantum-mechanical observable, which can be measured *via* X-ray diffraction techniques and can be calculated by first-principle methods. Numerous studies have been performed in an effort to compare the topologies found by these two approaches. In an overwhelming majority of cases, the experimental and theoretical topologies are identical (Koritsanszky & Coppens, 2001). Furthermore, as both techniques have advanced, the values of the charge density measured by the two approaches have converged (Farrugia & Evans, 2005; Arnold *et al.*, 2000). We expect this trend to continue and in the near future there will be negligible difference between calculated and measured charge densities. This fact can be used to great effect in the fields of materials science and condensed matter physics, where accurate density functional theory (DFT) calculations have become routine. Given this fact, it becomes plausible to use first-principle methods to uncover structure property relationships, which are then subject to experimental confirmation.

Incorporating first-principles methods into the discovery process could accelerate the pace of scientific understanding and technological advance. As an example, here we compare the topologies of two h.c.p. elements, Zr and Ru, by way of first-principles calculations. Surprisingly, while the crystal structure of the two metals is identical, we find that their

PHYSICAL REVIEW LETTERS

Topology of the Spin-Polarized Charge Density in bcc and fcc Iron

Travis E. Jones,[1,][*] Mark E. Eberhart,[1] and Dennis P. Clougherty[1,2]

[1]*Molecular Theory Group, Department of Chemistry and Geochemistry, Colorado School of Mines, Golden, Colorado 80401, USA*
[2]*Department of Physics, University of Vermont, Burlington, Vermont 05405-0125, USA*

We report the first investigation of the topology of spin-polarized charge density, specifically in bcc and fcc iron. While the total spin-density is found to possess the topology of the non-magnetic prototypical structures, the spin-polarized charge densities of bcc and high-spin fcc iron are atypical. In these cases, the two spin densities are correlated: the spin-minority electrons have directional bond paths and deep minima, while the spin-majority electrons fill these holes, reducing bond directionality. The presence of distinct spin topologies allows us to show that the two phase changes seen in fcc iron (paramagnetic to low-spin and low-spin to high-spin) are different. The former follows the Landau symmetry-breaking paradigm and proceeds without a topological transformation, while the latter involves a topological catastrophe.

Bader's topological theory of molecular structure, Atoms in Molecules (AIM), has been successfully applied to a variety of crystalline systems [1–9]. It has been employed to investigate the nature of bonding in materials ranging from high temperature alloys to biological systems. These have yielded surprising results, such as second neighbor bond paths in B2 ionic crystals [3] and transition metal aluminides [4], with the magnitude of the latter correlating to failure properties [5]. Other studies have used bond path properties to offer first principles explanations of stress-induced failure in brittle and ductile alloys [6], as well as shear elastic constants in a variety of pure metals and alloys [7,8]. Building on these ideas and using the rigorous definitions of bond paths afforded by the theory, the anomalous behavior of iridium under shear was also explained [9].

One of the attractive features of AIM is its reliance on the charge density, a quantum mechanical observable, that is most often calculated but can, in principle, be measured via x-ray diffraction techniques [10]. In a similar fashion, the spin-polarized charge density is an observable that can be calculated or measured using spin-polarized neutron diffraction. Despite the information and insights that have come from topological investigations of the total charge density, the same analysis has yet to be performed on spin-polarized densities. Here, we report the results from the first such studies, exploring the spin-minority and spin-majority topologies of body-centered-cubic (bcc) and face-centered-cubic (fcc) iron.

This first application of AIM to spin density sheds light on the origins of the magnetic phase transitions of fcc iron. It is argued that this system undergoes two distinct phase transitions during volume expansion: a second-order phase change, from a paramagnetic to a low-spin state, occurs at smaller volumes. It is coincident with a change in the charge density at the critical points without a topological transformation. At larger volumes, the low-spin state changes to high-spin through a discontinuity in the mo-

ment, where the topology also transforms. Thus, the latter change is a topological phase transition.

The framework of AIM can be applied in the same manner to both the total and spin-polarized densities. It is known from the Hohenberg-Kohn theorem that all ground-state molecular properties are a consequence of its charge density $\rho(\vec{r})$ [11], a scalar field in three spatial dimensions. Bader noted $\rho(\vec{r})$ must also contain the essence of a molecule's structure, which can be described topologically.

The topology of a general scalar field can be characterized in terms of its critical points (CPs), the zeros of the gradient of this field. There are four kinds of CP in a three-dimensional space: a local minimum, a local maximum, and two kinds of saddle points. These CPs are conventionally denoted by an index, which is the number of positive curvatures minus the number of negative curvatures. For example, a minimum CP has positive curvature in three orthogonal directions; therefore, it is called a (3, 3) CP. The first number is simply the number of dimensions of the space, and the second number is the net number of positive curvatures. A maximum is denoted by (3, −3), since all three curvatures are negative. A saddle point with two of the three curvatures negative is denoted (3, −1), while the other saddle point is a (3, 1) CP.

Through extensive studies of molecules and crystals, Bader [1] and Zou and Bader [2] showed that it was possible to correlate topological properties of the charge density with elements of molecular structure and bonding. In particular, a bond path was shown to correlate with the ridge of maximum charge density connecting two nuclei, such that the density along this path is a maximum with respect to any neighboring path. The existence of such a ridge is guaranteed by the presence of a (3, −1) CP between bound nuclei. As such, this CP is sometimes referred to as a bond CP.

Other types of CPs have been correlated with other features of molecular structure. A (3, 1) CP is topologically required at the center of ring structures, e.g., benzene.

The irreducible bundle: Further structure in the kinetic energy distribution

Travis E. Jones[a)] and Mark E. Eberhart

Molecular Theory Group, Colorado School of Mines, Golden, Colorado 80401, USA

Modern molecular sciences are often concerned with the properties and dynamics of chemical bonds. With the ability to experimentally measure charge density, there is a pressing need to find the relationships between charge density and the properties of chemical bonds. Here we show molecules can be partitioned into unique bond volumes characterized by well defined properties. Moreover, this partitioning recovers unrecognized structure in the kinetic energy distribution. © *2009 American Institute of Physics.* [DOI: 10.1063/1.3139113]

It is common practice to rationalize an atomic system's behaviors as arising from the properties of its constituent chemical bonds. To give but three examples, Gao *et al.*[1] predicted that the hardness of crystal surfaces results from a number of bond related properties including bond energy; the unusual dynamics of water molecules confined in single-walled nanotubes have been attributed to "pliable" bonds;[2] and Fujimori *et al.*[3] employed synchrotron radiation powder data to determine the strength of the intra-/intercluster bonds in α-rhombohedral boron. What should be surprising is that for these investigations—and countless others—the bond is not treated as a physical observable. In fact, there are some who suggest that the bond cannot be observed as it does not exist.[4,5] Until recently, this speculation was largely academic, as it was impossible to observe molecular charge density in sufficient detail to resolve the issue. However, with the application of improved high resolution diffraction techniques, this is no longer the case.[6] Now, if they exist, bonds can be detected and many of their properties measured.

The possibility that one could observe bond breaking, forming, and rearranging during chemical and physical processes has provided the impetus for research seeking to uncover relationships between the bonds of molecular or condensed phase systems and their properties. By default, the results of these investigation are framed around a topological description of molecular structure, atoms in molecules (AIMs),[7] which decomposes the total and spin resolved[8] charge density into atomic basins connected by bond paths. It is the unambiguous assignment of bond paths that makes AIM the preferred approach by which to glean bonding-property relationships in fields as diverse as metallurgy[9] and biophysics.[10,11] While AIM formalism can ascribe topological properties to the bond, it sheds no light on the more important question—the existence of bonds as structures possessing quantifiable properties. Here, we will show that AIM theory may be extended to include such structures.

AIM derives part of its validity from Hohenberg–Kohn theorem, which posits that all ground-state molecular properties are a consequence of the charge density, a scalar field denoted here as $\rho(\vec{r})$.[12] Bader noted that $\rho(\vec{r})$ must also contain the essence of a molecule's structure, which can be described topologically in terms of its critical points (CPs)—the zeros of the gradient of this field. There are four kinds of CP in a three-dimensional (3D) space: A local minimum, a local maximum, and two kinds of saddle point. These CPs are denoted by the number of positive curvatures minus the number of negative curvatures. For example, a minimum CP has positive curvature in three orthogonal directions and is called a (3, 3) CP. The first number is simply the number of dimensions of the space, and the second number is the net number of positive curvatures. A maximum is denoted by $(3, -3)$ since all three curvatures are negative. A saddle point with two negative curvatures is denoted $(3, -1)$, while the other saddle point is a (3, 1) CP.

Bader and co-worker[7,13] demonstrated that it is possible to correlate topological properties of $\rho(\vec{r})$ with elements of molecular structure. The ridge of maximum charge density connecting two nuclei was found to correlate with the occurrence of a "chemical bond" and was called a *bond path*. Such a ridge is guaranteed by the presence of a $(3, -1)$ CP, justifying its designation as a bond CP. A (3, 1) CP is required at the center of ring structures and is designated a ring CP. Cage structures are characterized by a (3, 3) CP, earning its designation as a cage CP. Moreover an atomic nucleus coincides with a maximum, a $(3, -3)$ CP, and hence is often referred to as a nuclear CP.

It was further demonstrated that there are regions containing a single nucleus for which properties are well defined. A necessary condition for delineating these regions is that they be bounded by a surface of zero flux in the gradient of the charge density (referred to here as zero-flux surfaces or ZFSs). Because there is a unique ZFS bounding every nuclear CP, one can find, for example, the energy of each region and sum these to give the molecular energy. This is exactly the property expected of the "atoms in a molecule." The key is that properties can be associated with any region bounded by a ZFS, and nuclear CPs are always bounded by a unique ZFS.

Defining bonds is more problematic, as there are an infinite number of ZFSs surrounding every bond CP and every bond path. Hence, it was thought that bond properties could

130, 204108-1

First-principles study of the mode-1 fracture of Fe-TiX interfaces (X=C,N)

Travis E. Jones,[*] Matt A. Sauer, and Mark E. Eberhart

Molecular Theory Group, Colorado School of Mines, Golden, Colorado 80401, USA

(Received 29 February 2008; published 8 September 2008)

We compare the evolution of the charge density in mode-1 fracture with that in uniaxial separation of two model systems: coherent Fe-TiC and Fe-TiN interfaces. These charge densities were calculated using both band structure and cluster codes. The topology of charge density in the cluster calculations converged with that of the bulk within two coordination spheres. Furthermore, we found that the topology of initial and final states is independent of the applied strain. However, the topological evolution is strain dependent. While we observed one topological catastrophe in Fe-TiC, independent of strain, we saw two separate catastrophes under uniaxial separation of Fe-TiN and only one under mode-1 fracture. This behavior suggests that there is some kinetic control mediating fracture in these iron-ceramic interfaces.

Brittle failure is an important phenomenon that is believed to be controlled by interactions at the tip of atomically sharp cracks.[1] In an effort to gain insight into fractures' atomic scale mechanism and ultimately limit its costly consequences, many investigators have turned to first-principles methods. However, due to symmetry breaking and complex crack tip reconstruction, quantitative calculations of even simple cleavage process are computationally intractable. Hence, rather than modeling fracture directly, most studies have been concerned with calculating pertinent thermodynamic parameters such as the ideal work of adhesion.[2] The kinetic aspects of fracture have been all but ignored, even though some have suggested that fracture may have a kinetic component and, if so, would be subjected to kinetic control.[3,4] Our objective is to assess this possibility.

In this study we have modeled decohesion in two idealized systems: coherent Fe-TiC and Fe-TiN interfaces. Our goal is to determine how the charge redistribution accompanying fracture is influenced by chemistry and fracture path. What makes this approach unique is that the charge redistribution is described topologically, allowing us to identify topological transition states (TTSs) along the chosen fracture path. Once identified, we are able to apply the Hammond postulate and make rough estimates of the comparative energies of path- and chemistry-dependent transition states.

The Hammond postulate[5] was first articulated in 1955 and became one of the most cited articles of the Journal of the American Chemical Society (over 3000 cites to date). Hammond proposed that for two similar reactions, the one in which the transition state comes earlier in the process will be the one preferred. This postulate is quite general and, in principle, can be applied to condensed phase phenomena. In 1982, Whitesides[4] stressed that the conceptual framework of chemistry, particularly transition state theory and the Hammond postulate, may have applications in the study of deformation and fracture.

To exploit the Hammond postulate we appeal to Bader's[6] topological theory of molecular structure, atoms in molecules. It is known from the Hohenberg-Kohn theorem that a system's ground-state properties are a consequence of its charge density, a scalar field denoted here as $\rho(\vec{r})$.[7] Bader noted that the essence of a molecule's structure must be contained within the topology of $\rho(\vec{r})$. The topology of a scalar field, in this case $\rho(\vec{r})$, is given in terms of its critical points (CPs), which are the zeros of the gradient of this field. There are four kinds of CPs in a three-dimensional space: a local minimum, a local maximum, and two kinds of saddle points. These CPs are denoted by an index, which is the number of positive curvatures minus the number of negative curvatures. For example, a minimum CP has positive curvature in three orthogonal directions; therefore, it is called a (3,3) CP. The first number is simply the number of dimensions of the space, and the second number is the net number of positive curvatures. A maximum is denoted by $(3,-3)$, since all three curvatures are negative. A saddle point with two of the three curvatures negative is denoted $(3,-1)$, while the other saddle point is a (3,1) CP.

Through extensive studies of molecules and crystals, Bader[6] showed that it was possible to correlate topological properties of the charge density with elements of molecular structure and bonding. A maximum, a $(3,-3)$ CP, is always found to coincide with the atomic nucleus, and so it is called an atom CP. But of greater importance, a bond path was shown to correlate with the ridge of maximum charge density connecting two nuclei such that the density along this path is a maximum with respect to any neighboring path. The existence of such a ridge is guaranteed by the presence of a $(3,-1)$ CP between nuclei. As such, this critical point is often referred to as a bond CP. Other types of CPs have been correlated with other features of molecular structure. A (3,1) CP is required at the center of ring structures. Accordingly, this CP is designated a ring CP. Cage structures are characterized by a single (3,3) CP within the cage, and again, these CPs are given the descriptive name of cage CPs.

With a description of molecular structure in terms of the topology of $\rho(\vec{r})$, it is possible to represent fracture in terms of the topological evolution of $\rho(\vec{r})$. Those points where the topology of $\rho(\vec{r})$ changes, i.e., at catastrophes, will correspond to TTSs. By the Hammond postulate, the relative energy of these states can be assessed.

Calculations were performed with both VASP (Ref. 8) and Amsterdam density functional (ADF).[9] We made use of the Perdew-Wang 91 generalized gradient corrections.[10] The calculations consisted of two parts: (1) building clusters that

The Bond Bundle in Open Systems

TRAVIS E. JONES, MARK E. EBERHART

Molecular Theory Group, Colorado School of Mines, Golden, CO 80401

ABSTRACT: Much of modern chemistry is concerned with the properties and dynamics of chemical bonds. Although they have been described variously, the most familiar representation is that of a link connecting two atoms. However, no one has yet developed a scheme by which to partition a molecule into bond volumes with well-defined properties. As a consequence, the chemical bond is left as nothing more than a heuristic devise. Here, we show molecules can be partitioned into bond-bundles–volumes that share many of the properties associated with the conceptual bond. This partitioning follows naturally through an extension of Baders topological theory of molecular structure. Surprisingly, it also bounds regions of space containing nonbonding or lone-pair electrons and leads to bond orders consistent with those expected from theories of directed valance. © 2009 Wiley Periodicals, Inc. Int J Quantum Chem 110: 1500–1505, 2010

Key words: bonds; atoms in molecules; bond bundle

Introduction

With the ability to observe condensed phase and molecular structure at finer scales comes the desire to rationalize properties in terms of charge density, a quantum mechanical observable [1]. Bader's topological theory of molecular structure, atoms in molecules (AIM) allows the charge density to be decomposed into atom points and bond paths, making such investigations more compatible with traditional chemical ideas [2]. The ability to unambiguously define hydrogen [3] and dihydrogen bonds [4], as well as other weak interactions [5], has made this technique popular in fields as diverse as metallurgy [6] and biophysics [7, 8]. Although these studies are able to show that two atoms have the topological properties associated with linked atoms, they are unable to associate well-defined properties to those links. Here, we show molecules can be partitioned into bond volumes with well-defined properties through an extension of AIM theory.

The topological theory of molecular structure derives part of its validity from Hohenberg–Kohn theorem, which posits that all ground-state molecular properties are a consequence of the charge density, a scalar field denoted here as $\rho(\vec{r})$ [9]. Bader [2] noted that $\rho(\vec{r})$ must also contain the essence of a molecule's structure, which can be described topologically in terms of its critical points (CPs)— the zeros of the gradient of this field. There are four kinds of CP in a three-dimensional space: a local minimum, a local maximum, and two kinds of saddle point. These CPs are denoted by an index, which is the number of positive curvatures minus the number

The Visualization and
Use of Electronic Structure
for
Metallurgical Applications

ABSTRACT

While the application of electronic structure theory has significantly impacted many areas of technology, including those concerned with materials development, it has not proved to be a truly useful tool of the metallurgist. We believe that this is a consequence of the specialized concepts and vocabulary in which the results of electronic structure calculations are framed and communicated. These specialized concepts have not been integrated easily into the metallurgical tool kit, which makes primary use of structure property relationships. In this paper, we present a new way of visualizing the electronic structure of a metal or alloy. This approach extends the concept of crystal structure, making it a continuous variable of quantum mechanically determined parameters of the charge density. Using the B2 transition metal-aluminides as examples, we also show that there are relationships between this extended concept of structure and the phase stability of a modeled alloy. As structure can be viewed as a function of continuous variables, it is possible to determine the distance from one structure to another and from one structure to its point of instability i.e. its phase boundary. We argue that this distance is manifest physically in terms of a metal or alloy's elastic constants.

Topological Catastrophe and Isostructural Phase Transition in Calcium

Travis E. Jones[†],* Mark E. Eberhart[†], and Dennis P. Clougherty[†‡]

[†] *Molecular Theory Group, Colorado School of Mines, Golden, Colorado 80401 and*
[‡] *Department of Physics, University of Vermont, Burlington, Vermont 05405-0125*
(Dated: December 6, 2010)

We predict a quantum phase transition in fcc Ca under hydrostatic pressure. Using density functional theory, we find at pressures below 80 kbar, the topology of the electron charge density is characterized by nearest neighbor atoms connected through bifurcated bond paths and deep minima in the octahedral holes. At pressures above 80 kbar, the atoms bond through non-nuclear maxima that form in the octahedral holes. This topological change in the charge density softens the C' elastic modulus of fcc Ca, while C_{44} remains unchanged. We propose an order parameter based on applying Morse theory to the charge density, and we show that near the critical point it follows the expected mean-field scaling law with reduced pressure.

PACS numbers:

The theory and characterization of solid-solid isostructural phase transitions has been an area of intense experimental and theoretical research since they were described in 1949 [1]. What sets these transitions apart from others is that while crystalline properties change–sometimes discontinuously–crystallographic structure does not, making these transitions purely electronic in nature. Both first order and continuous transitions are known to exist. A well known example of the former is the $\gamma \to \alpha$ transition in fcc Ce [1], while a magneto-volume instability in fcc Fe is an example of the later [2].

In the case of Fe, the traditional local order parameter, μ, gave conflicting results computationally, with the transition appearing as first [3] or second [2] order. It was not until the transition was interpreted as a topological change of the electronic charge density, $\rho(\vec{r})$, that the underlying nature of the phase change became apparent [4]. While this approach is promising, no general correlations have been drawn between isostructural phase transitions and $\rho(\vec{r})$. We use this approach to predict an isostructural phase transition in calcium under hydrostatic pressure. We then apply Morse theory to the charge density and propose an order parameter for the transition. We show that this order parameter scales in the appropriate way with reduced pressure near the quantum critical point.

One of the advantages of casting theories of isostructural phase transition in terms of $\rho(\vec{r})$ is that it is a quantum observable. Though $\rho(\vec{r})$ is often calculated by way of first principles methods (e.g. density functional theory (DFT)), the total charge density can also be measured via X-ray diffraction techniques, and the spin-polarized charge density can be determined using spin-polarized neutron diffraction. As it is also known that all ground state properties depend on the charge density [5], it seems appropriate to seek relationships between the structure of $\rho(\vec{r})$, changes to that structure, and corresponding changes to properties. We note that previous work has proposed that DFT could be used as a general framework for analyzing quantum phase transitions in electronic systems [6].

The electron charge density is a 3 dimensional scalar field. Morse theory tells us the charge density can be characterized by its rank 3 critical points (CPs), the points at which the gradient of the field vanishes. There are four kinds of rank 3 CP in a three-dimensional space: a local minimum, a local maximum and two kinds of saddle point. These are conventionally denoted by an index, which is the number of positive curvatures minus the number of negative curvatures. For example, a minimum CP has positive curvature in three orthogonal directions; therefore it is called a (3, +3) CP. The first number is the dimensionality of the space, and the second number is the net number of positive curvatures. A maximum is denoted by (3, -3), since all three curvatures are negative. A saddle point with two of the three curvatures negative is denoted (3, -1), while the other saddle point is a (3, +1) CP.

Through extensive studies of molecules and crystals, Bader and Zou showed that it was possible to correlate topological properties of $\rho(\vec{r})$ with elements of molecular structure and bonding [7, 8]. In particular, a bond path was shown to correlate with the ridge of maximum charge density connecting two nuclei. The existence of such a ridge is guaranteed by the presence of a (3, -1) CP. As such, this CP is often referred to as a bond CP. Other types of CPs have been correlated with other features of molecular structure. A (3, +1) CP is topologically required at the center of ring structures. Accordingly, it is designated a ring CP. Cage structures must enclose a single (3, +3) CP and are given the name cage CPs. The locations of the atomic nuclei always coincide with a (3, -3) CP. Hence, it is often called an atom or nuclear CP.

In this study, the charge density of fcc Ca was calculated at various lattice constants and strains using the Vienna *ab-initio* Simulation Package (VASP) version 4.6 [9]. All calculations were performed with the Perdew-

---

*Electronic address: `trjones@mines.edu`

Convergence of density functional iterative procedures with a Newton-Raphson algorithm

J. W. Jerome · P. R. Sievert · L.-H. Ye · I. G. Kim · A. J. Freeman

Abstract State of the art first-principles calculations of electronic structures aim at finding the ground state electronic density distribution. The performance of such methodologies is determined by the effectiveness of the iterative solution of the nonlinear density functional Kohn-Sham equations. We first outline a solution strategy based on the Newton-Raphson method. A form of the algorithm is then applied to the simplest and earliest density functional model, i.e., the atomic Thomas-Fermi model. For the neutral atom, we demonstrate the effectiveness of a charge conserving Newton-Raphson iterative method for the computation, which is independent of the starting guess; it converges rapidly, even for a randomly selected normalized starting density.

Keywords Density functional theory · Kohn-Sham system · Newton-Raphson algorithm · Thomas-Fermi model

1 Introduction

Traditional mixing methods for density functional theory calculations may not be appropriate for the larger complex systems of current technological interest. Mixing employs successive approximation iterates of a fixed point mapping. Such iterates are often found to converge very slowly or not at all.

J. W. Jerome (✉)
Department of Mathematics, Northwestern University, Evanston, IL 60208, USA
e-mail: jwj@math.northwestern.edu

P. R. Sievert · L.-H. Ye · I. G. Kim · A. J. Freeman
Department of Physics and Astronomy, Northwestern University, Evanston, IL 60208, USA
e-mail: art@freeman.phys.northwestern.edu

Currently, mixing is employed at the level of the nonlinear discretization equations (see Ref. [1] for a discussion of Anderson mixing, Broyden updates, and the relation between them). Here an operator version of the Newton-Raphson method, applied to the Kohn-Sham system of density functional theory, is suggested.

2 Density functional theory

We are interested in the application of density functional theory to periodic structures in solid-state physics. A development of the Kohn-Sham system, as derived from the Hohenberg-Kohn theorem, is presented in Ref. [2]. The theory represents a many-electron system in terms of non-interacting effective particles; the inter-electron effects are transferred to the exchange-correlation potential, expressed as a functional of the electron density ρ. The Coulomb potential is also determined in terms of ρ and the fixed nuclear charge. The consolidated potential is the effective potential V_{eff}. This leads to the Hamiltonian H and its associated Kohn-Sham orbitals. We thus obtain the operator representation of the Kohn-Sham system as described specifically below. The operator (structure map) is linearized in our application of the Newton-Raphson method, and can be incorporated into existing electronic structure codes (see Ref. [3]).

3 Structure map

The structure map may be represented schematically as a mapping P for the self-consistent Kohn-Sham equations. It is defined on possible electron density configurations, satisfying charge conservation laws. A solution of the Kohn-Sham system is a fixed point ρ, so that $P\rho = \rho$. The mapping P

Convergence of Density Functional Iterative Procedures with a Newton-Raphson Algorithm

J.W. JEROME

Department of Mathematics, Northwestern University, Evanston, IL 60208 USA

jwj@math.northwestern.edu

P.R. SIEVERT, L.-H. YE, I.G. KIM, and A.J. FREEMAN

Department of Physics and Astronomy, Northwestern University, Evanston, IL 60208 USA

art@freeman.phys.northwestern.edu

Abstract. State of the art first-principles calculations of electronic structures aim at finding the ground state electronic density distribution. The performance of such methodologies is determined by the effectiveness of the iterative solution of the nonlinear density functional Kohn-Sham equations. We first outline a solution strategy based on the Newton-Raphson method. A form of the algorithm is then applied to the simplest and earliest density functional model, i.e., the atomic Thomas-Fermi model. For the neutral atom, we demonstrate the effectiveness of a charge conserving Newton-Raphson iterative method for the computation, which is independent of the starting guess; it converges rapidly, even for a randomly selected normalized starting density.

Keywords: Density functional theory, Kohn-Sham system, Newton-Raphson algorithm, Thomas-Fermi model

1. Introduction

Traditional mixing methods for density functional theory calculations may not be appropriate for the larger complex systems of current technological interest. Mixing employs successive approximation iterates of a fixed point mapping. Such iterates are often found to converge very slowly or not at all. Currently, mixing is employed at the level of the nonlinear discretization equations (see Ref. [1] for a discussion of Anderson mixing, Broyden updates, and the relation between them). Here an operator version of the Newton-Raphson method, applied to the Kohn-Sham system of density functional theory, is suggested.

2. Density Functional Theory

We are interested in the application of density functional theory to periodic structures in solid-state physics. A development of the Kohn-Sham system,

as derived from the Hohenberg-Kohn theorem, is presented in Ref. [2]. The theory represents a many-electron system in terms of non-interacting effective particles; the inter-electron effects are transferred to the exchange-correlation potential, expressed as a functional of the electron density ρ. The Coulomb potential is also determined in terms of ρ and the fixed nuclear charge. The consolidated potential is the effective potential V_{eff}. This leads to the Hamiltonian H and its associated Kohn-Sham orbitals. We thus obtain the operator representation of the Kohn-Sham system as described specifically below. The operator (structure map) is linearized in our application of the Newton-Raphson method, and can be incorporated into existing electronic structure codes (see Ref. [3]).

3. Structure Map

The structure map may be represented schematically as a mapping P for the self-consistent Kohn-Sham

Strong interface adhesion in Fe/TiC

J.-H. LEE*†, T. SHISHIDOU‡, Y.-J. ZHAO§, A. J. FREEMAN† and G. B. OLSON¶

†Department of Physics and Astronomy, Northwestern University,
Evanston, IL 60208, USA
‡Department of Quantum Matter, ADSM, Hiroshima University,
Higashihiroshima, 739-8530, Japan
§NanoStellar Inc., Menlo Park, CA 94025, USA
¶Department of Materials Science and Engineering, Northwestern University,
Evanston, IL 60208, USA

As an aid to understanding the superior toughness of Ti-modified steels provided by fine $Ti(C, N)$ particles, first-principles full-potential linearized augmented plane wave (FLAPW) density functional calculations were performed on the Fe matrix/TiC particle interface. It was found that at equilibrium a strong covalent bonding between Fe–C is formed at the interface, and the magnetic moment of the interface Fe $(1.98\,\mu_B)$ is reduced from that of the tetragonally strained structure $(2.51\,\mu_B)$. We then calculated with a rigid separation model the separation energy curve and the force separation law for the Fe–C debonding process at the interface, which predicts $2.45\,J\,m^{-2}$ for the work of separation and 30.66 [GPa] for the force maximum. We also found that the strong Fe–C bond provides an interfacial fracture strength equal to that of the pure bcc Fe matrix. A clear picture is given for the microscopic origin of this strong metal/ceramic adhesion based on density of states (DOS) considerations. For a more realistic understanding of the Fe–C bonding, structural optimization calculations were performed at each separation distance. The effect of relaxation was found to be larger at short separation distances than in the large separation region, which leads to a crossover behavior in the separation energy curve from the elastically deformed to the clearly separated regime at a critical distance ($\sim 1.75\,\text{Å}$), and to a discontinuity in the force separation law. Despite this large relaxation effect, the work of separation, $2.52\,J\,m^{-2}$, is not changed much from that of rigid separation.

1. Introduction

The ultimate goal of steel research is to design new classes of high performance steels [1] with sufficient advances in fracture toughness and strength to visibly increase component life with minimal increase in cost. To this end, the control of dispersed inclusion phases within the Fe-based matrix plays a crucial role. It has been

---

*Corresponding author. Email: jhyoung73@northwestern.edu